Towards creating a set of Battery Mineral Reference Materials
for Applied Mineralogy and Mineral Processing Research

Part 1: Nickel Reference Materials

By

Alan R Butcher
Professor of Geomaterials & Applied Mineralogy, GTK

With contributions from

Ester M Jolis*, Sari Lukkari*, Pasi Heikkilä*, Ted Nuorivaara*, Radoslaw M Michallik*, Simon P Michaux*, Lorenza Sardisco#, Nikolaos Apeiranthitis$, Max Franzel$, Jesal Hirani#, Johanna Tepsell+ and Tim J Pearce+$

*Geological Survey of Finland (GTK)

+X-ray Mineral Services Oy (XMSF), #X-ray Mineral Services Ltd (UK) & $Hafren Scientific Group

GTK Open File Work Report

BATCircle 2.0

April 23, 2023

GEOLOGICAL SURVEY OF FINLAND   DOCUMENTATION PAGE

28 April 2023

Authors Butcher et al	Type of report GTK Open File Work Report
	Commissioned by Business Finland

Title of report
Towards creating a set of Battery Mineral Reference Materials for Applied Mineralogy and Mineral Processing Research   Part 1: Nickel Reference Materials

Abstract
See Summary

Keywords
Reference Material, battery minerals, drill core, nickel concentrate, QXRD, SEM-EDS, EPMA, ICP-OES, ICP-MS XRF, scanning micro-XRF, Raman, LIBS, FTIR

Other information
The work is part of the BATCircle2.0 Project, funded by Business Finland

Report serial GTK Open File Work Report	Archive code 26/2023

Total pages 44	Language English	Price NA	Confidentiality Public

Unit Circular Economy Solutions	Project code 50404-40210210

Name/signature Jouko Nieminen	Signature/name Alan R Butcher

BATCircle 2.0

April 23, 2023

April 23, 2023

Contents   **PAGE**

April 23, 2023

Summary

This study documents the geochemical and mineralogical characteristics of three **Nickel Reference Materials**, and forms part of **Work Package 5**, Circular Battery Materials Value System, as part of **BATCircle 2.0 Project**, in collaboration with partners **Aalto University** and **VTT**. This is Part 1 of four deliverables, with others covering similar reports on Lithium and Cobalt Reference Materials, along with recommendations for an e-Waste Reference Material.

The new **Reference Materials** reported here comprise ¼ **Drill Cores** of typical nickel-rich ores, cm-sized chips of **Run-of-Mine** ore, and finely ground **Nickel Concentrate**, all from the same deposit. Together, they are not designed to be definitive mineral or rock standards, but rather represent samples that have been characterized using multiple methods (optical, e-beam, x-ray beam, laser-beam), at different scales (cm-micron), and in different forms (drill core, crushed and milled ore, thin-section, polished block).

It is the intention that the new data and physical sub-samples will be made available to all those within the **BATCircle 2.0 Consortium** who are interested in battery mineral research. Typical end-users for the new materials might include: geologists, mineralogists and material scientists interested in testing new analytical or experimental devices; or minerals engineers that require well-characterized materials for flotation, leaching or physical separation experiments.

A novel aspect of the study is that we have used both traditional geoanalytical techniques for battery mineral characterization (whole rock geochemistry, QXRD, SEM-EDS, EPMA, Automated Mineralogy), as well as new and emerging technologies (scanning micro-XRF, LIBS, FTIR, Raman), thus creating a unqiue set of data for the three sample types, including new spectral information which can be used for building mineral identification libraries. Some of the devices used are handheld and are sufficiently portable that they can be operated efficiently in the field, which opens up the possibility of wider use, leading to new applications in earth and mineral sciences.

The results, whether they be chemical, mineral or textural in nature, largely correlate across the different techniques. This report aims only to document the findings rather than interpret them, as this activity will form the basis of a planned scientific journal paper, which will compare the relative accuracy and precision of the results across all 4 commodities (Ni-Li-Co-eWaste).

A further planned output from the present study is a quick reference **Fact Sheet** that will accompany each **Reference Material** before they are dispatched to researchers. This will be published separately once the materials are ready for release.

April 28, 2023

1　CONTEXT

This report summarises research carried out to date by the **Geological Survey of Finland** (**GTK**), within Work Package 5 (**WP5**), Circular Battery Materials Value System, as part of an on-going **Business Finland**-funded Project, known as **BATCircle 2.0**, in collaboration with partners **Aalto University** and **VTT**. The specific and relevant objectives of **WP5** are as follows:

- Extensive characterization of battery materials from both **Primary** and **Secondary** sources

- Development of **Reference Materials** for **Li**, **Co** and **Ni**

- Assessment of how to develop an **e-waste** materials characterization reference material

In order to fulfill these objectives, the following tasks are underway:

- **Task 5.3.1**
  Development of **Reference Materials** for **Nickel**, **Lithium** and **Cobalt**

- **Task 5.3.2**
  Assessment to plan the development of characterization of **Reference Electronic Waste**

Four reports are planned, each covering one of the main topics within Tasks 5.3.1 and 5.3.2. The present report documents the results for a new **Nickel Reference Material**, and is labelled accordingly as **Part 1** (of 4).

2　CONCEPT

The original idea was to create a collection of well-characterized materials that could be used by researchers, whether they be geologists, mineralogists, geochemists, mineral processors, or any other professions linked to battery minerals, metals, and materials. Ideally, we wanted to characterize ores (drill cores or hand samples, or run-of mine material), processed products (concentrates), and final materials (saleable products), and make sub-samples of these available to all those interested, along with a fact sheet. For some commodities (Li) we have collected a near complete set of samples. Cobalt is proving to be challenging but we are progressing well. In the case of nickel, the subject of the present report, we have secured samples of drill core, crushed run-of-mine ore, and nickel concentrate. And finally, a bulk sample of e-waste that has been delivered to GTK, is currently awaiting investigation, and will be reported at later date.

3　STANDARD REFERENCE MATERIAL VS REFERENCE MATERIAL

At the commencement of the **BATCircle 2.0 Project**, we wanted to clarify the meaning of the following terms, Standard, Standard Reference Material, and Reference Material.

April 28, 2023

A **Standard** is generally defined (at least in the world of analytical geomaterials) as a material (say crystal, mineral, rock type) with absolute known values that can be used for calibrating analytical techniques & instrumentation. It is usually available in the form of a fine powder, or a single crystal or grain, which tends to limit the variability of the standard from sub-sample to sub-sample during manufacture.

On the other hand, a **Standard Reference Material** (again, in the context of analytical geomaterials) is a general term for a so-called *round-robin* material, which is specifically manufactured to be analysed by multiple laboratories in order to establish intra- and inter-laboratory variation, in terms of accuracy, precision, and general variance in results, especially when comparing the same technology (say ICP or XRF), or different technologies (say XRD, SEM and EPMA).

Our preferred terminology, and the one used in the present study, is simply to refer to these types of materials in this study as **Reference Materials**. By using this short descriptor, we imply that materials have been specifically created with scientific and engineering research in mind. These **Reference Materials**, although well-characterized (in terms of their bulk geochemical composition, known mineral content and textures, and other material properties), will display natural variation, from batch to batch, because of their very nature (drill cores, ore lumps, and processed mineral particles), and so cannot be considered as true **Standards**.

Multiple batches of **Reference Material** will be manufactured as aliquots from a Master sample, and made available, in the first instance at least, to members of the **BATCircle 2.0 Consortium**, and then later to interested parties outside, depending on demand and availability of material. Each batch will be accompanied by a **Fact Sheet**, which we believe will be adequate to allow the recipient to plan and design their own experiments, and is certainly an excellent starting point for any further research on them. Ideally, additional analytical work on these batches would then be fed back to the GTK and incorporated into documentation of any future batches. The kinds of uses we envisage for these **Reference Materials** might include, but are not restricted to, the following: teaching, research, professional development, fingerprinting (tracking and tracing), general metallurgical testing, and technology testing.

4   GEOANALYTICAL TECHNIQUES USED TO CHARACTERIZE THE REFERENCE MATERIALS

There are a bewildering number of analytical techniques that are currently available to geologists when it comes to the characterization of drill cores, crushed core and particulate mineral products. These include: optical methods (petrographic microscopy); X-ray analysis (XRF, XRD, X-CT), electron-beam analysis (SEM, EPMA) and laser-based techniques (LA-ICP-MS, Raman, LIBS) and others (FTIR). In this report, we document many of these for a suite of nickel-bearing **Reference Materials** sampled from a single Ni (Cu) deposit in Finland.

April 28, 2023

5   DETAIL OF MASTER SAMPLES USED TO MAKE THE NICKEL REFERENCE MATERIALS

5.1   Types of samples

Three types of nickel-bearing samples form the basis of the **Nickel Reference Material**, all from the same deposit (Boliden's Kevitsa Mine, Finland – referred to hereafter as the Company), as follows:

- **Drill Cores**

These comprise quarter drill core sections, sampled from GTK's historic Kevitsa drill hole material at our **National Core Archive** in Loppi, and were selected based on their general representative nature of typical nickel-bearing ores. The actual drill cores sampled for this study came from various drill hole intersections within the ore deposit, with differing grades of ore, and identified by the Company as: high-grade; medium-high grade; and low grade. Specifically, the whole rock geochemistry, QXRD and Automated Mineralogy was performed on quarter core sections from drill hole 3714/R367, which was drilled in 1992, and were taken from core tray L-25, (hence full identification as M52/3714/92/R367/L-25). Other techniques such as micro-XRF were performed on quarter drill cores from L-29, L-39, L40, and L-41.

- **Run-of-Mine Ore** lumps

Samples of typical Run-of-Mine Ore (ROM), partially crushed, as sampled from a conveyor at the active mine, and are typically made up of cm-sized lumps, as sampled by the Company, on CVR 4 at 08:30 on 10 June 2022. Particle sizes are highly variable, and can be as large as 15 mm, but typically around 5-10 mm, along with particles smaller in diameter.

- **Nickel Concentrate**

This material is an example of Nickel Concentrate (NFC), as sampled by the Company on 10 June 2022, and appears as medium to dark grey powder, with occasional agglomerations up to 2cm in diameter.
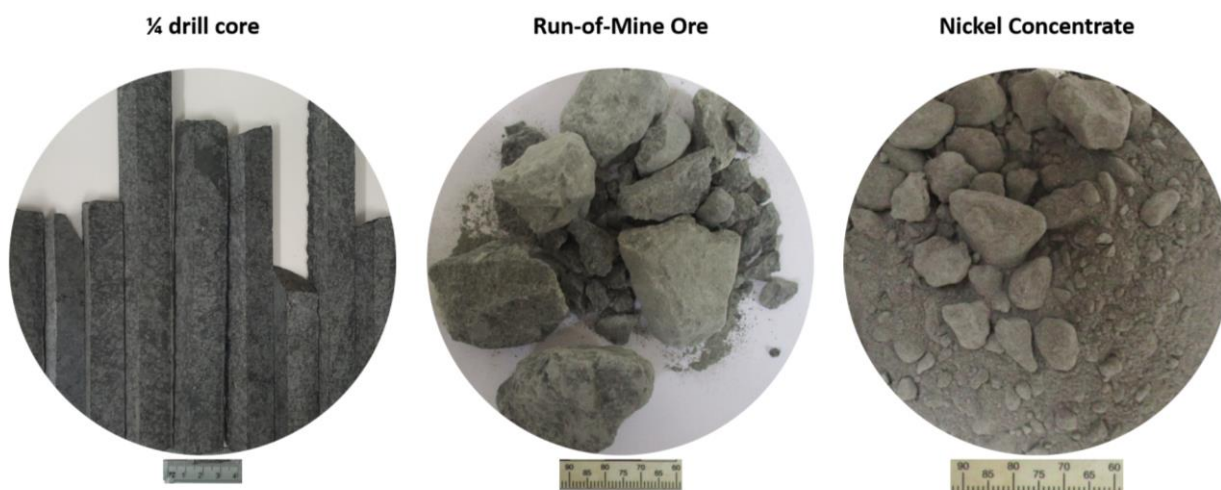

Figure 1.
Three types of samples make up the **Nickel Reference Material** set: ¼ drill core, Run-of-Mine ore, & Nickel Concentrate.

6   CHARACTERIZATION OF THE NICKEL REFERENCE MATERIALS

6.1   Background

X-ray Fluorescence Spectrometry (**XRF**) is a standard method of analysis in order to gain a bulk geochemical analysis of any geomaterial. It is ideal for major elements, some minor elements, but is generally unsuitable for trace and ultra-trace elements. The sample is typically required to be in the form of pressed powdered pellets or glass beads.

Inductively Coupled Plasma Optical Emission spectroscopy (**ICP-OES**) is generally considered a superior method for multi-elemental analysis over XRF, for both major and minor elements, but is only suitable for some trace elements.

Inductively Coupled Plasma Mass Spectrometry (**ICP-MS**) is used typically only for trace elements, and can analyse, if required, down to detection limits of parts per billion. It is especially useful for quantifying rare earth elements.

LECO analysis is named after an acronym of the original name of the developers (**L**aboratory **E**quipment **Co**rporation), and is for organic and inorganic materials through sample combustion and measurement of combustion gas absorption, as seen in the infrared region of the electromagnetic spectrum. Typically used for determining sulphur, carbon in ore samples, but can also be used for nitrogen, oxygen, and hydrogen determinations.

X-ray diffraction is a robust whole-rock analytical technique for identifying minerals and phases present in a sample, based on their characteristic diffraction patterns, and when used in conjunction with specialised software, the **Rietveld method** allows for quantitative modal analysis (**QXRD**). Minerals present in low quantities (5 vol% or less) can be problematic for QXRD. Some minerals display overlapping diffractograms, leading to challenging identifications. The technique relies on the ability to determine the crystallinity of the mineral for a positive identification to be made, and therefore amorphous minerals are therefore problematic. Sample needs to be pulverized to a fine powder.

Scanning micro-XRF is a non-invasive, x-ray beam source, elemental and mineralogical analysis technique that is relatively new and still being adopted by the mining industry. It can map rock samples and powdered materials, with best results obtained from a flat 2D surface. When combined with off-line petrographic software, that uses elemental information returned from secondary X-ray signals processed by dual EDS detectors, quantitative mineral chemical and textural analysis and mapping is possible. Drill core samples can be measured in their entirety (up to 15 cm long), producing maps that cover areas greater than a traditional polished surface, such as a polished thin section or polished block (typically 2 -5 cm), which are invaluable for creating contextural mineral maps. The beam interaction volume is around 20 microns in diameter, with a minimum spatial resolution possible down to 5 microns.

Automated Mineralogy is an established method to map 2D polished surface of samples by Scanning Electron Microcopy using Energy Dispersive Spectrometry (**SEM-EDS**) to determine micro-composition, and to create mineral maps with textural details that allow for quantification of grain sizes, shapes, and associations. Grain boundaries, inclusions, and fractures can also be mapped. The sample is usually presented to the instrument in the form of a thin section or polished block. Scanning resolution can be down to as little as 1 micron, but typically a stepping interval greater than this is used to speed up measurement time.

Electron microprobe analysis (**EMPA**) is the most common and widely used non-destructive method for quantified micro-chemical analysis of minerals and solid materials utilizing the wavelength-dispersive spectrometry (**WDS**) technique. Most commonly used for spot analysis with the smallest spatial resolution of one to a few micrometers, recent developments allow also for sub-micrometer scale measurements as well as relatively quick quantified 2D mapping and profile analysis. WDS-EPMA is an important complementary technique for LA-ICP-MS quantified analysis, with a detection limit of a few 100 ppm, but cannot measure ultralight elements such a Li, Be, H and He.

Raman spectroscopy (**Raman**) is a non-destructive mineral analysis technique which provides detailed information about chemical structure, phase identification and crystallinity. It is based upon the interaction of light with the chemical bonds within a material, following interaction with a laser beam focused onto the surface of a sample.

Laser Induced Breakdown Spectroscopy (**LIBS**) is a technology gaining momentum in the mining industry after having much success in the oil and gas sector. The laser is focussed to form a plasma which atomizes and excites the sample under investigation. Typically used in field portable devices. Certain elements found in particular minerals respond well to LIBS, such as Li in spodumene. It was used in this study as an experimental method.

Fourier Transform Infra-Red spectroscopy (**FTIR**) uses a monochromatic beam of light and measures how much of the light is absorbed, and the algorithm used to calculate this (taking raw data and making it into a spectrum that can be interpreted for mineralogical information) is known as the Fourier Transform. It was used in this study as an experimental method.

7   RESULTS FOR NICKEL REFERENCE MATERIALS

7.1   Whole-rock multi-element geochemical analysis - XRF, ICP-OES, ICP-MS

The results of whole-rock analysis of **¼ drill core**, **Run-of-Mine Ore**, and **Nickel Concentrate** are provided in **Tables 1a-f**.

They are arranged according to the methods used, which include:

Table 1a: Comparison of **ICP-OES** and **ED-XRF**, major oxides only

Table 1b: Comparison of **ICP-OES** and **ED-XRF**, minor and trace elements only

Table 1c: Additional trace elements by **ED-XRF**

Table 1d. Additional trace elements by **ICP-MS**

Table 1e. Trace elements by external laboratory (**ICP-MS** and **XRF**), for comparison

Table 1f. **LECO sulphur** and **carbon** analysis, by external laboratory.

Further details of the methods used can be found in the **Appendix**. Gold and the PGMs were not analysed for.

April 28, 2023

Table 1a. Major elements as oxides by ICP-OES and ED-XRF.

ICP-OES

Method	Sample ID	Al2O3	SiO2	TiO2	Fe2O3	MnO	MgO	CaO	Na2O	K2O	P2O5	Total
BatCirc2-Ni-ICP	Drill core	2.37	42.07	0.24	15.90	0.18	23.56	10.50	0.43	0.09	0.02	95.36
BatCirc2-Ni-ICP	ROM ore	3.21	46.84	0.36	10.11	0.14	19.76	15.55	0.58	0.17	0.02	96.73
BatCirc2-Ni-ICP	Ni concentrate	0.55	15.52	0.07	45.29	0.04	7.05	2.34	0.15	0.07	0.00	71.09

ED-XRF

Method	Sample ID	Al2O3	SiO2	TiO2	Fe2O3	MnO	MgO	CaO	Na2O	K2O	P2O5	Total
BatCirc2-Ni-XRFs	Drill core	2.37	38.84	0.22	15.70	0.17	27.76	9.36	<0.13	0.05	<0.00069	94.47
BatCirc2-Ni-XRFs	ROM ore	3.05	41.30	0.35	10.19	0.13	23.00	14.04	<0.13	0.18	<0.00069	92.24
BatCirc2-Ni-XRFs	Ni concentrate	0.98	31.74	0.12	55.55	0.01	19.32	2.94	<0.13	0.10	<0.00069	110.76

Table 1b. Minor & trace elements in ppm by ICP-OES and ED-XRF.

ICP-OES

Method	Sample ID	Ba	Ce	Cr	Cu	La	Nb	Ni	Sc	Sr	Th	V	Y	U	Zn	Zr
BatCirc2-Ni-ICP	Drill core	30.52	82.19	3249.36	4596.23	0.00	0.00	3527.33	40.67	32.11	21.16	125.77	6.53	6.65	133.30	15.08
BatCirc2-Ni-ICP	ROM ore	33.81	99.11	2461.28	1897.25	8.46	0.00	2563.87	55.86	50.56	11.56	153.06	15.24	4.98	76.42	22.39
BatCirc2-Ni-ICP	Ni concentrate	8.39	55.81	582.37	2077.52	0.00	0.00	47992.45	6.55	19.38	60.56	65.79	1.67	13.75	433.01	15.38

ED-XRF

Method	Sample ID	Ba	Ce	Cr	Cu	La	Nb	Ni	Sc	Sr	Th	V	Y	U	Zn	Zr
BatCirc2-Ni-XRFs	Drill core	38.60		2640.00	6289.00	17.50	1.90	3089.00		19.40	1.20	66.50	7.60	1.40	96.30	13.40
BatCirc2-Ni-XRFs	ROM ore	45.80		2355.00	1574.00	18.60	2.00	1993.00		39.70	1.70	127.10	17.40	1.10	50.10	23.60
BatCirc2-Ni-XRFs	Ni concentrate	<6.0		870.40	12230.00	23.90	6.30	47305.92		8.80	11.60	<5.0	5.80	5.90	452.20	<0.2

Table 1c. Additional trace elements in ppm by ED-XRF.

ED-XRF

Method	Sample ID	Be	Co	Cs	Dy	Er	Eu	Ga	Gd	Hf	Ho	Lu	Mo	Nd	Pb	Pr	Rb	Sm	Sn	Ta	Tb	Tl	Tm	W	Yb
BatCirc2-Ni-XRFs	Drill core		88.30	10.90				<1.6		63.30			2.8		6.10		2.20		<1.5	0.10				<1.5	
BatCirc2-Ni-XRFs	ROM ore		55.90	9.40				<1.4		17.10			2.9		4.40		5.80		2.00	13.90				<1.3	
BatCirc2-Ni-XRFs	Ni concentrate		1671.00	<14				<3.3		457.00			22.8		<0.5		4.00		<3.0	1181.00				61.30	

Table 1d. Additional Trace elements in ppm by ICP-MS.

ICP-MS

Method	Sample ID	Ba	Ce	Cr	Cu	La	Nb	Ni	Sc	Sr	Th	V	Y	U	Zn	Zr
ICP-MS	Drill core	35.74	4.65	3321.53	4603.99	1.92	1.26			28.55	0.53	130.39	5.86	0.17	127.18	16.06
ICP-MS	ROM ore	42.17	27.27	2539.20	1885.71	10.96	1.20			49.77	1.03	164.80	15.15	0.27	72.01	23.41
ICP-MS	Ni concentrate	9.26	1.94	590.79	2003.73	0.91	0.80			14.76	0.82	68.02	2.31	0.30	415.42	15.99

ICP-MS

Method	Sample ID	Be	Co	Cs	Dy	Er	Eu	Ga	Gd	Hf	Ho	Lu	Mo	Nd	Pb	Pr	Rb	Sm	Sn	Ta	Tb	Tl	Tm	W	Yb
ICP-MS	Drill core	0.69	207.83	0.31	0.99	0.54	0.30	5.01	1.07	0.60	0.24	0.07	9.78	4.82	18.12	0.65	2.77	0.89	2.43	0.18	0.18	0.11	0.23	52.52	0.59
ICP-MS	ROM ore	0.52	127.04	0.42	3.08	1.48	0.61	5.63	3.51	0.86	0.61	0.18	3.36	20.50	11.20	4.42	6.22	3.95	2.20	0.15	0.52	0.08	0.33	53.72	1.31
ICP-MS	Ni concentrate	0.61	2523.86	0.28	0.29	0.14	0.05	1.59	0.31	0.52	0.08	0.03	11.25	2.81	19.85	0.27	3.46	0.30	2.06	0.11	0.05	0.04	0.14	53.53	0.20

Table 1e. Trace elements in ppm by XRF and ICP-MS, as supplied from an external laboratory, for comparison.

External Lab

Method	Sample ID	Ba	Ce	Cr	Cu	La	Nb	Ni	Sc	Sr	Th	V	Y	U	Zn	Zr
XRF/ICP	Drill core	14	1	2510	5714	<1	1	2652	1	20	<10	80	<1	<10	54	2
XRF/ICP	ROM ore	21	2	2520	1399	1	2	1477	1	50	<10	150	1	<10	37	30
XRF/ICP	Ni concentrate	5	2	430	8162	<1	1	>10000	1	4	<10	88	<1	<10	424	4

External Lab

Method	Sample ID	Be	Co	Cs	Dy	Er	Eu	Ga	Gd	Hf	Ho	Lu	Mo	Nd	Pb	Pr	Rb	Sm	Sn	Ta	Tb	Tl	Tm	W	Yb
XRF/ICP	Drill core	<1	121		<1	<1	<1	6	<1	<1	1	<1	9	1	<1	<1	1	<1	1	<1	<1	<1	<1	<1	<1
XRF/ICP	ROM ore	<1	58		<1	<1	<1	4	<1	<1	1	<1	8	1	3	<1	1	<1	1	<1	<1	<1	<1	<1	<1
XRF/ICP	Ni concentrate	<1	2245		<1	<1	<1	19	<1	<1	3	3	1	31	<1	1	2	1	<1	<1	5	<1	<1	<1	<1

Table 1f. Sulphur and carbon analysis by the LECO method, as supplied by an external laboratory.

External Lab

Method	Sample ID	C	S
XRF/ICP	Drill core	0.19	2.37
XRF/ICP	ROM ore	0.15	0.88
XRF/ICP	Ni concentrate	0.19	25.36

April 28, 2023

7.2   QXRD - Mineralogical analysis

Quantitative X-ray Diffraction (**QXRD**) was carried out on representative examples of all three **Nickel Reference Materials**. The **Rietveld Method** was used to quantify the mineral percentages, using **AutoQuan** software.

It should be noted that **pentlandite** and **chalcopyrite** have awkwardly overlapping peaks in their diffractograms, and this can lead to challenges in quantification, especially when pentlandite is abundant, as in the case of the Nickel Concentrate. Serpentine is a highly-orientated mineral (fibrous and platy), and is therefore also difficult to fully quantify by QXRD, but the variety present is likely to be lizardite. Talc is also a tricky mineral by QXRD, and even though the values must be viewed with caution, they are considered to be largely reliable.

Table 2. **QXRD** results, expressed as a weight percent, for each mineral phase identified.

Sample	Chlorite	Quartz	Plagioclase	Pyroxene	Olivine	Actinolite	Talc	Serpentine	Pentlandite	Pyrrhotite	Magnetite	Pyrite	Total
Drill core	8.5	0.8	1.8	32.5	17.2	28.4	TR	5.4	0.7	4.8	0.0	TR	100
ROM ore	10.5	1.1	4.5	43.0	5.3	26.1	TR	1.3	0.7	1.2	0.0	0.3	100
Ni-concentrate	4.5	0.2	0.0	4.1	0.0	1.9	16.8	0.0	22.6	45.7	1.9	2.3	100

A comparison to the whole-rock geochemistry results can be found in the **Appendix**, along with further details of the sample preparation techniques used in the characterization of these samples.

7.3   Scanning micro-XRF - Whole-core micro-chemical, mineral & texture imaging & analysis

Scanning Micro-XRF was used in this study to analyse representative drill cores and create mineral, elemental and textural distribution maps, in a non-invasive way. The main focus was to map the nickel-bearing minerals, and to reveal, at the core-scale, their distribution and associations.

With this in mind, three different **Drill Cores** were specifically chosen mainly because they represent examples of High-grade, Medium-grade and Low-grade, in terms of overall average grade (Ni-Cu), as classified by the Company.

The results, shown in **Figures 2 & 3**, are elemental maps coloured according to elemental abundances for ease of viewing. The maps appear to indicate that High-grade ore is associated mostly with localized cross-cutting sulphide-rich veins, whereas in the Medium- to Low-grade ores, the sulphides are disseminated and are largely interstitial to the silicates.

Further, it can be observed in all three ore types, that the distribution of the minerals of most economic interest (nickel- and copper-bearing phases, interpreted to be pentlandite and chalcopyrite, respectively), occur heterogeneously at the scale of a few mm-cm.

It should be noted that each batch of Nickel Reference Material Drill Core will be accompanied by a Fact Sheet, and although mostly will be of Medium-grade, all three may be present in any of the cores provided. Further images of similar Drill Cores are shown in the **Appendix**.

April 28, 2023
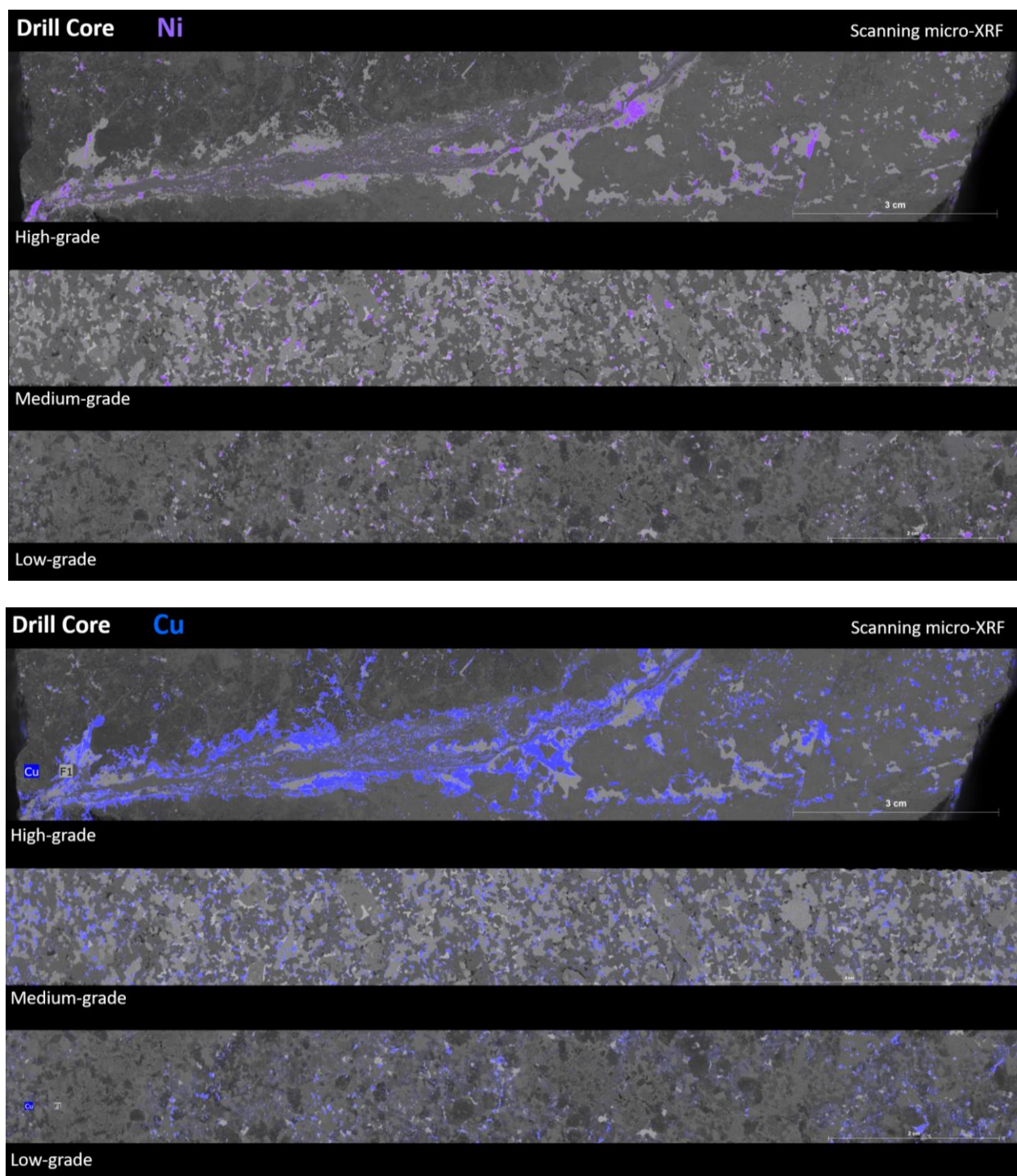
Figure 2.
Scanning Micro-XRF elemental maps of three different **Drill Cores**, specifically chosen because they represent ores of variable grade, from High-grade, through Medium-grade, to Low-grade. Maps are for nickel and copper distribution, which are proxies for pentlandite and chalcopyrite, respectively.
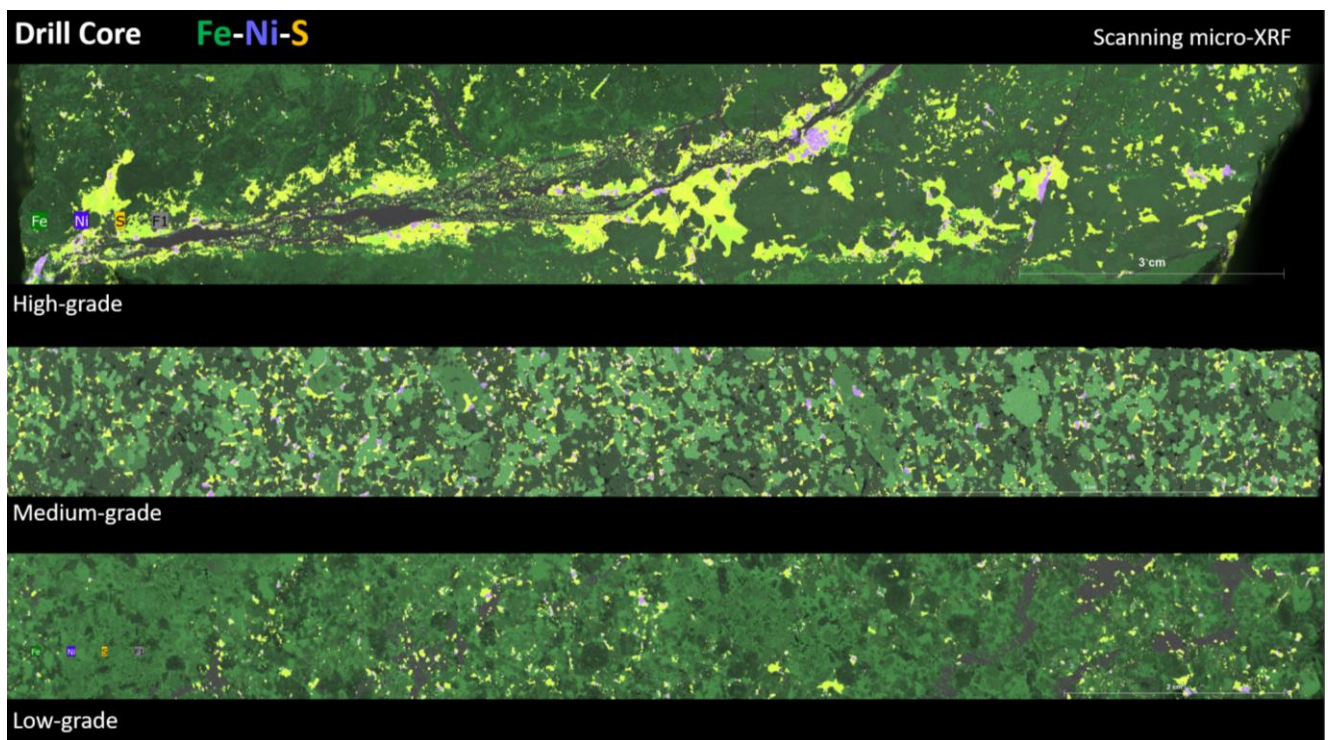
April 28, 2023

Figure 3.
Scanning Micro-XRF elemental maps of three different **Drill Cores** for iron, nickel and sulphur distribution, which allows for the pentlandite (purple colour) to be easily visualized.

April 28, 2023

7.4   Automated Mineralogy - Run-of-Mine Ore & Nickel Concentrate

Automated Mineralogy was performed on polished blocks prepared from representative **Run-of-Mine Ore** and aliquots of the **Nickel Concentrate**. Full details are provided in the **Appendix**.

7.4.1   Run-of-Mine Ore

The **Run-of-Mine Ore** samples used in this study comprised medium grey, fine to medium grained rock fragments, along with a coarsely crystalline rock fragment 15-20cm across (**Figure 4**).
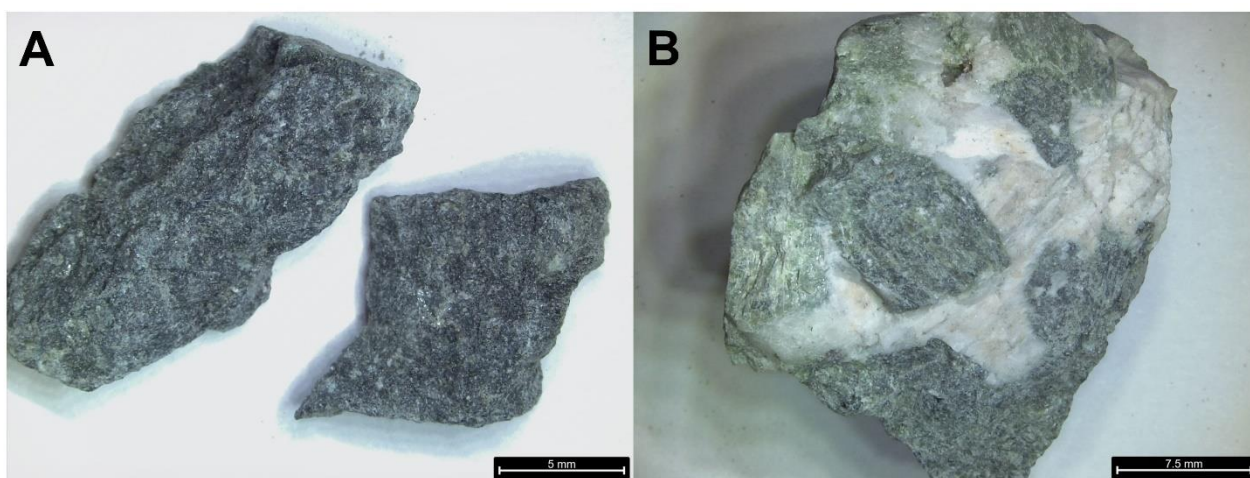
Figure 4.
Binocular microscope images of **Run-of-Mine Ore** fragments selected for polished resin impregnated blocks.

The modal compositions of the sub-samples are provided in **Table 3**, along with a repeat analysis of the more coarsely crystalline ore labelled as C.

April 28, 2023

Table 3. Quantitative modal abundance (area %) **ROM Ore** samples based on Automated Mineralogy.

Sample Name	Ni ROM Ore A	Ni ROM Ore B	Ni ROM Ore C
Quartz	0.03	0.00	0.00
K Feldspar	0.45	0.00	0.00
Plagioclase	4.59	0.08	0.01
Calcic Plagioclase	1.66	**11.41**	**11.92**
Muscovite	0.08	0.01	0.01
Biotite & Phlogopite	0.79	0.23	1.09
Chlorite & Vermiculite	2.15	4.92	8.59
Olivine	0.00	17.57	1.85
Orthopyroxene	0.03	12.91	12.51
Serpentine	0.01	12.46	26.14
Clinopyroxene	67.25	1.89	10.49
Clinopyroxene (Mid Al)	13.03	16.82	10.30
Clinopyroxene (High Al)	7.68	19.32	14.75
Zoisite	1.26	0.65	0.55
Calcite	0.28	0.04	0.04
Dolomite	0.35	0.07	0.04
Fe Oxides	0.00	0.77	0.78
Ti Oxides	0.30	0.29	0.24
Cr Spinel	0.00	0.28	0.47
Pyrite	0.01	0.02	0.01
Pyrrhotite	0.00	0.06	0.05
Chalcopyrite	**0.01**	**0.01**	**0.01**
Pentlandite	**0.02**	**0.04**	**0.03**
Sulphates & Phosphates	0.01	0.07	0.10
Undifferentiated	0.02	0.09	0.01

April 28, 2023

Modal abundance Ni ROM Ore
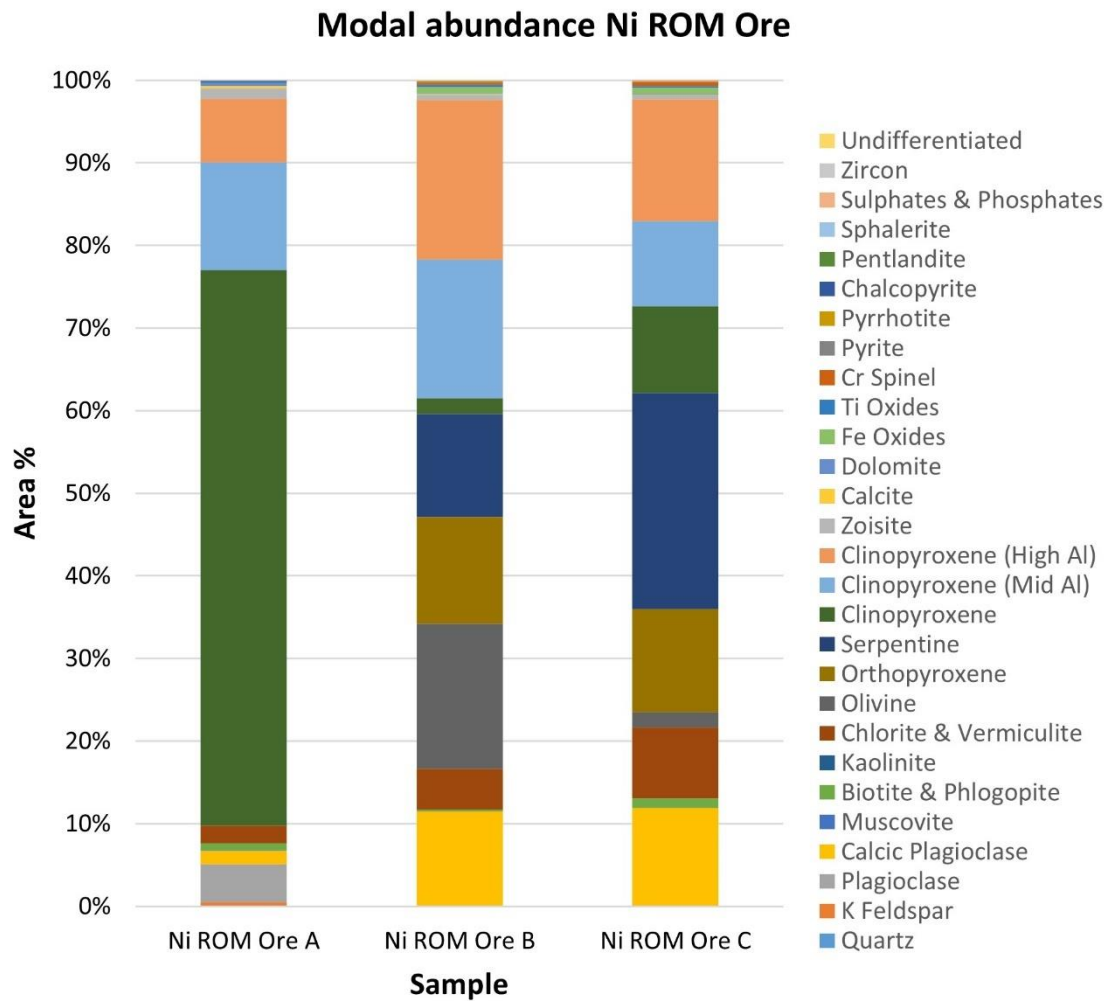
Figure 5.
Modal mineralogy for the **Run-of-Mine Ore** samples. Sample C is a second fragment of Sample B.

April 28, 2023
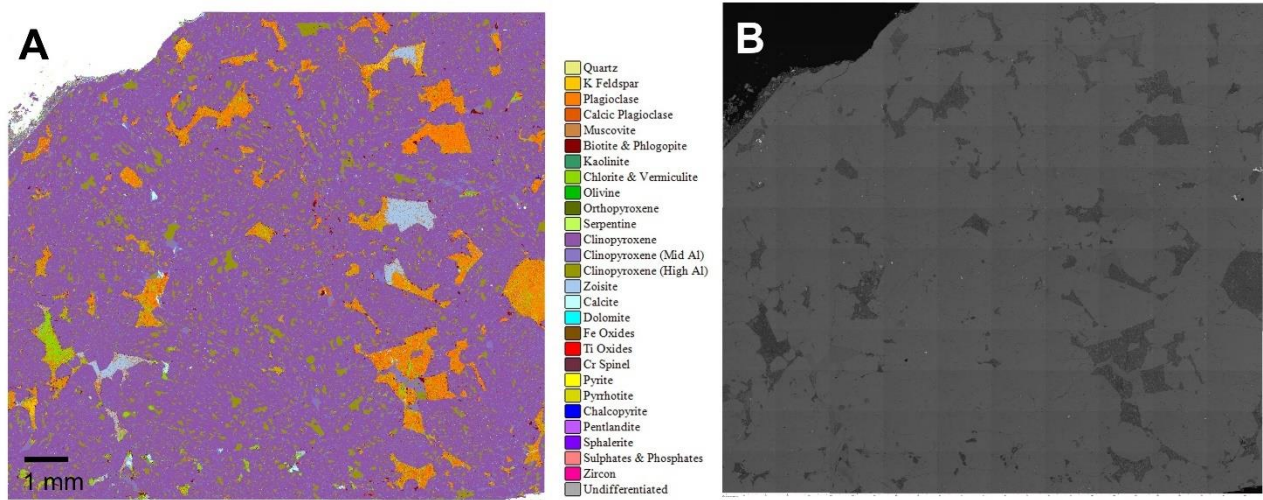
Figure 6.
Mineral maps. (A) AMICS and (B) SEM-BSE images for **Run-of-Mine Ore** chip, sub-sample A.
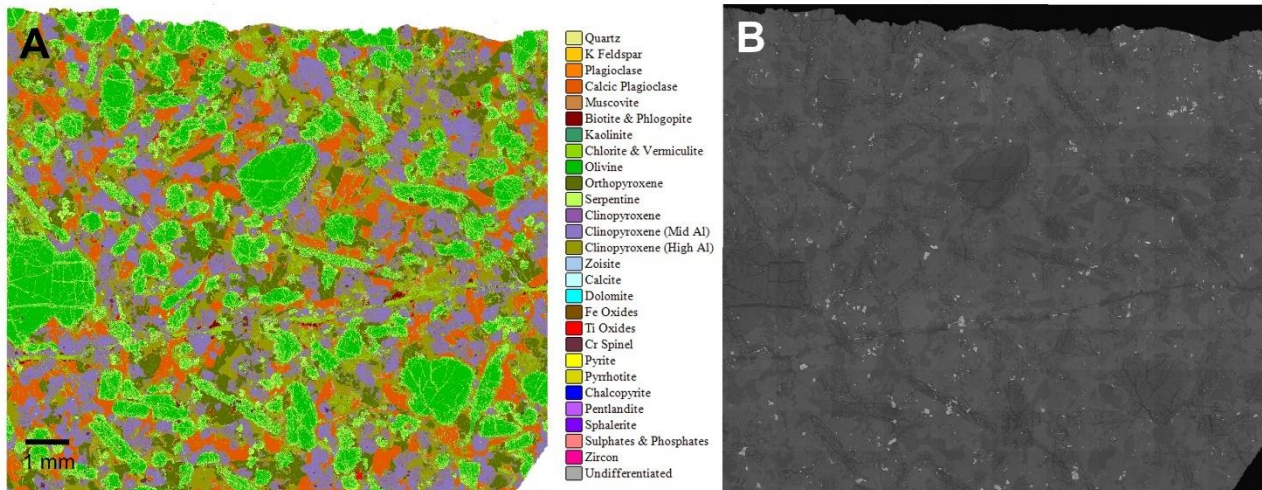
Figure 7.
Mineral maps. (A) AMICS and (B) SEM-BSE images for **Run-of-Mine Ore** chip, sub-sample B.

Grain size and association data are possible to calculate for these samples, but are not reported here given the low modal percentages of **pentlandite** & **chalcopyrite** in the chips, and these data can be better derived from the **Nickel Concentrate** results.

April 28, 2023

7.4.2   Nickel Concentrate

The modal compositions of two replicate blocks of the **Nickel Concentrate** sample are presented in **Table 4**.

Table 4. Modal composition of the two **Nickel Concentrate** replicate blocks, as determined by Automated Mineralogy.

Sample Name	Ni Conc A	Ni Conc B
Quartz	0.19	0.23
K Feldspar	0.00	0.01
Plagioclase	0.17	0.15
Calcic Plagioclase	0.08	0.07
Muscovite	0.00	0.01
Biotite & Phlogopite	1.02	1.17
Kaolinite	0.00	0.00
Chlorite & Vermiculite	3.15	3.90
Olivine	0.25	0.28
Orthopyroxene	22.92	24.48
Serpentine	1.35	1.29
Clinopyroxene	2.55	3.15
Clinopyroxene (Mid Al)	6.94	6.80
Clinopyroxene (High Al)	0.99	0.99
Zoisite	0.01	0.01
Calcite	0.30	0.29
Dolomite	0.56	0.58
Fe Oxides	0.83	0.81
Ti Oxides	0.04	0.05
Cr Spinel	0.04	0.03
Pyrite	4.94	5.06
Pyrrhotite	30.07	26.88
Chalcopyrite	2.49	2.41
Pentlandite	**20.81**	**21.05**
Sphalerite	0.03	0.03
Sulphates & Phosphates	0.16	0.17
Zircon	0.01	0.01
Undifferentiated	0.07	0.08
Total	100.00	100.00

GTK
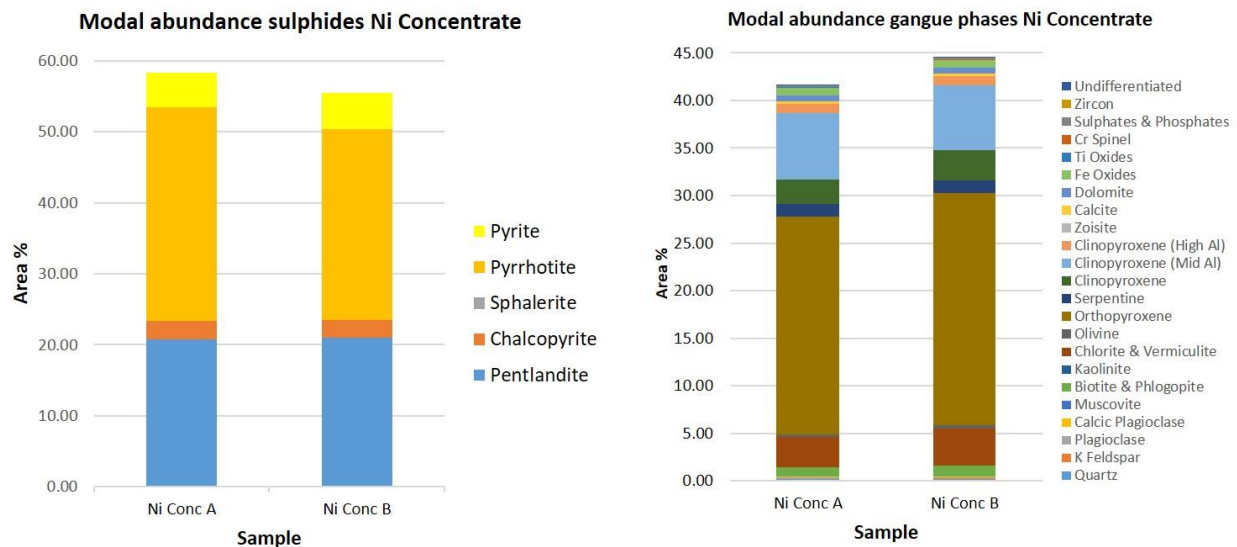
April 28, 2023

Figure 8.
Modal abundance of sulphide phases and gangue phases **Nickel Concentrate** replicates A & B.

April 28, 2023
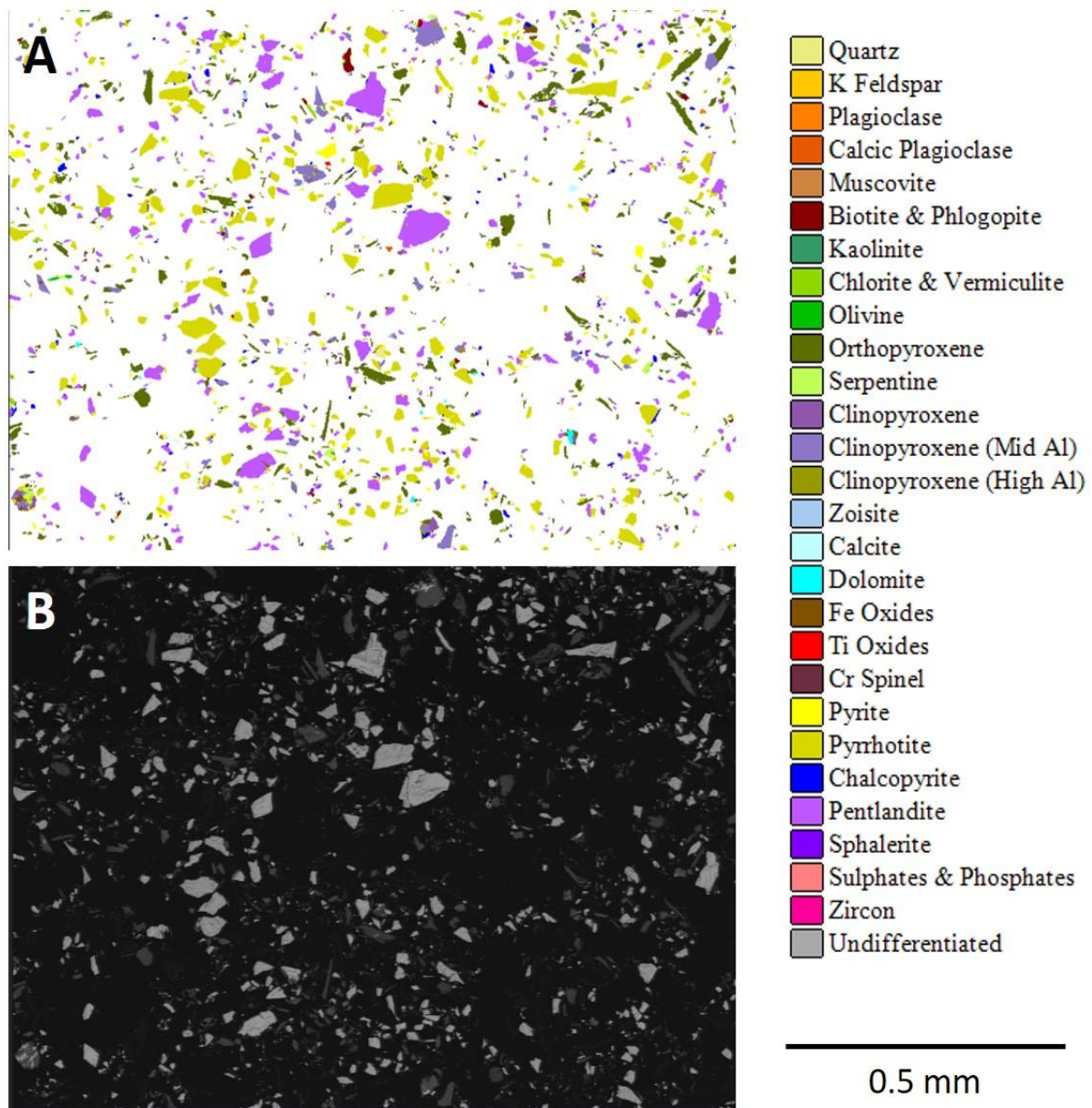
Figure 9.
Automated Mineralogy particle maps. (A) Enlarged area AMICS particle image **Nickel Concentrate** sample A and (B) corresponding area SEM-BSE image.

April 28, 2023
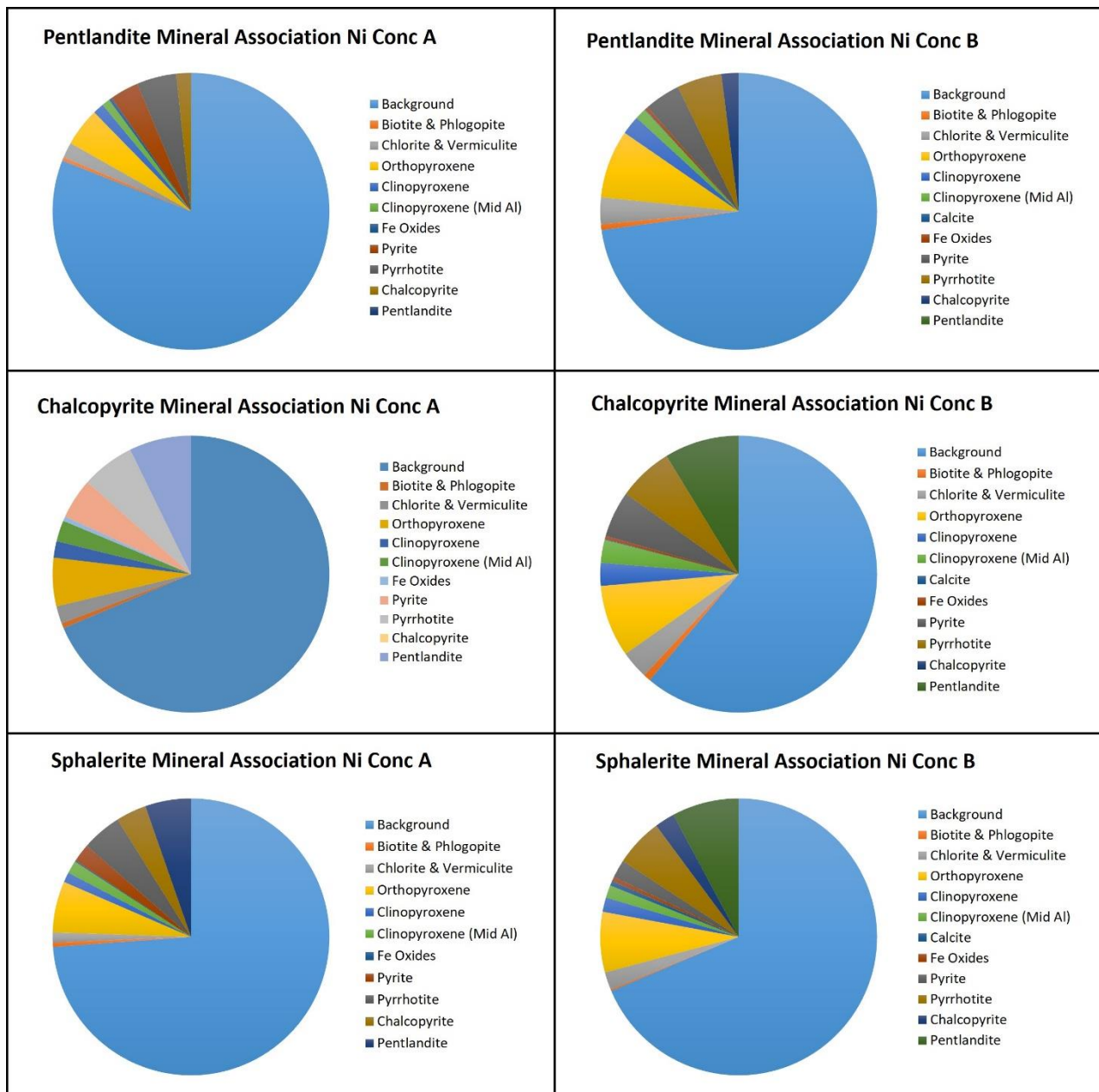
Figure 10.
Mineral association data for pentlandite, chalcopyrite and sphalerite for **Nickel Concentrate** subsamples A and B.

April 28, 2023

Table 5. Mineral liberation data for pentlandite, chalcopyrite and sphalerite in **Nickel Concentrate** subsamples A and B.

	A: Pentlandite	A: Chalcopyrite	A: Sphalerite	B: Pentlandite	B: Chalcopyrite	B: Sphalerite
0-5%	1	22	23	1	34	22
5-10%	1	9	5	1	8	5
10-15%	2	7	6	3	6	5
15-20%	4	5	3	14	5	2
20-25%	5	5	2	6	4	3
25-30%	3	4	3	2	3	2
30-35%	2	3	3	2	4	3
35-40%	2	3	5	2	3	1
40-45%	2	3	2	2	2	1
45-50%	2	3	1	2	2	4
50-55%	2	3	7	2	3	3
55-60%	2	3	2	2	2	0
60-65%	3	3	3	2	2	1
65-70%	3	3	6	3	2	2
70-75%	4	3	5	4	3	3
75-80%	5	3	1	4	2	5
80-85%	6	3	3	6	3	11
85-90%	9	4	3	7	2	2
90-95%	14	6	3	12	3	1
95-100%	27	7	15	25	7	23

Grain size data for **pentlandite**, **chalcopyrite** and **sphalerite** indicate that in the **Nickel Concentrate**, >65% of the pentlandite is less than 20 µm in size, >93% of the chalcopyrite is less than 20 µm in size and 86-100% of the sphalerite is less than 20 µm in size.

April 28, 2023

7.5   Quantitative micro-analysis – EPMA - Nickel Concentrate - SEM-EDS imaging

The aim of this exercise was twofold: to acquire high resolution images of the particles within the **Nickel Concentrate** sample; and to document the micro-chemical composition of the main nickel phase, pentlandite, and to investigate the level of nickel, as well as trace elements such as cobalt and copper. These observations therefore compliment the conventional whole-rock geochemistry, QXRD, and the Automated Mineralogy results. The sample was mounted in epoxy resin polished blocks to provide a flat analytical surface.

The results from quantitative analysis of 70 grains of pentlandite by Electron Probe Microanalysis (**EPMA**) are provide in **Table 6** below. **FEG-SEM** images of typical pentlandite-containing particle types are shown in **Figure 11**.

Table 6. **EPMA** analyses of typical pentlandite grains from the **Nickel Concentrate**. Of note, cobalt values are generally low but range from 0.46 – 4.33 weight percent. Nickel values are within expected ranges for pentlandite.

Weight%				
Fe	**Co**	**Ni**	**S**	**Total**
33.73	1.41	31.49	33.41	**100.06**
33.59	1.41	31.66	33.55	**100.23**
34.16	1.21	31.60	33.31	**100.27**
35.39	1.33	29.96	33.43	**100.14**
35.84	1.41	29.52	33.19	**99.96**
33.83	1.90	30.57	33.40	**99.74**
34.18	1.83	30.63	33.21	**99.86**
33.54	1.48	32.01	32.98	**100.02**
32.76	1.08	32.75	33.21	**99.80**
32.38	1.08	33.00	33.08	**99.58**
32.24	1.62	32.93	32.77	**99.59**
34.86	1.18	30.92	32.79	**99.80**
33.98	1.10	32.01	32.39	**99.50**
33.32	1.18	32.23	32.83	**99.58**
33.92	1.69	31.33	32.70	**99.69**
31.98	4.33	30.72	32.54	**99.57**
35.03	1.23	30.50	32.41	**99.21**
32.14	1.03	33.71	32.42	**99.31**
32.69	1.17	32.89	32.51	**99.27**
32.83	1.12	32.98	32.48	**99.45**
33.98	1.20	31.81	32.28	**99.28**
33.87	1.40	31.54	32.36	**99.18**
31.96	0.46	34.60	32.19	**99.21**
33.44	1.29	32.18	32.13	**99.03**
31.59	1.92	33.38	32.16	**99.11**
32.42	1.26	33.32	32.12	**99.14**

April 28, 2023
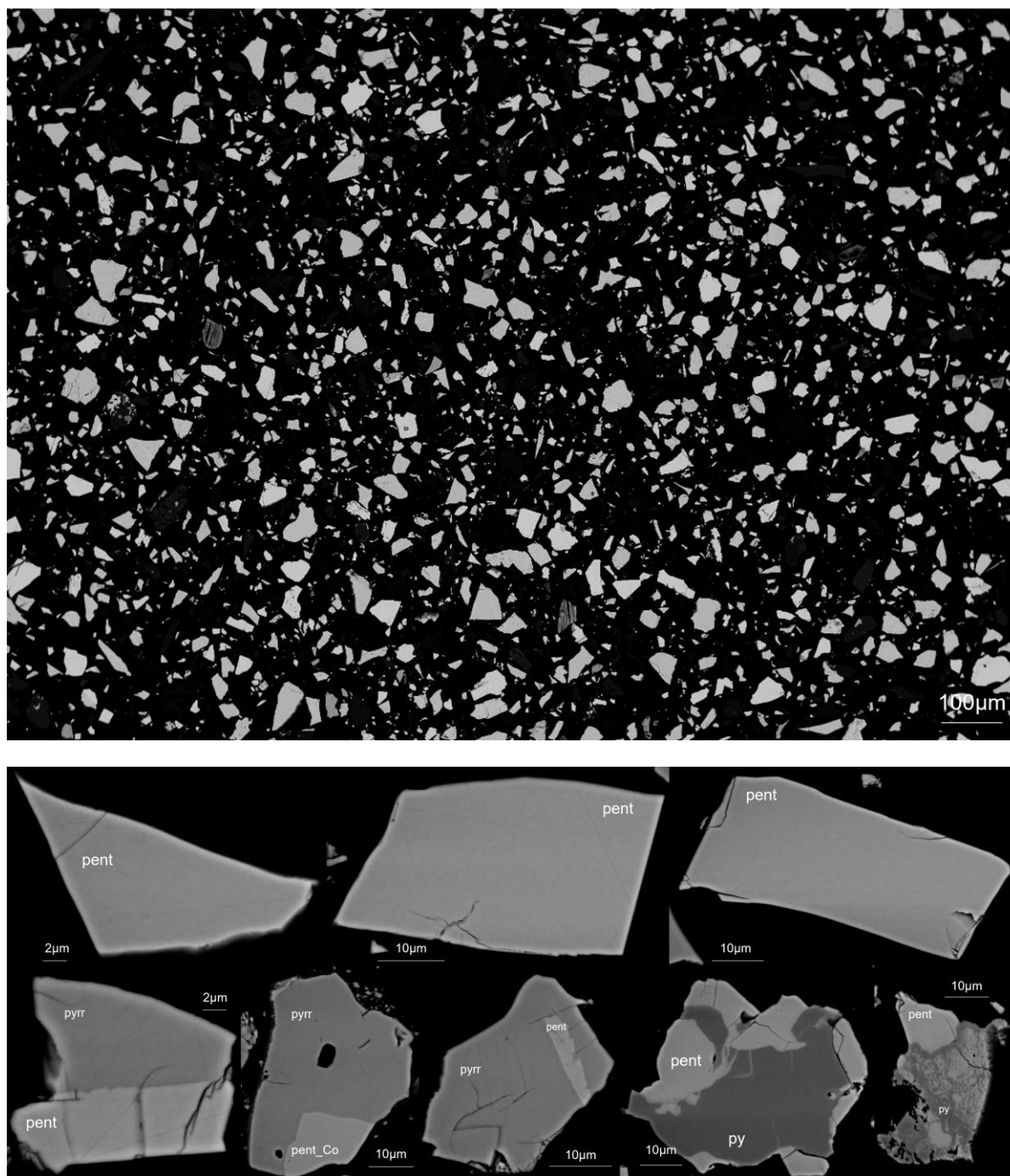
Figure 11.
Backscattered Electron Images of particles in the **Nickel Concentrate**, illustrating the types of particle present, with emphasis on the **pentlandite-bearing** ones. *Upper* image: general view of the particle population. *Lower image*: montage of typical particle types that contain pentlandite (abbreviated to pent, except where cobalt was detected by SEM-EDS, and then pen_Co). Locking with pyrrhotite (pyrr) and pyrite (pyr) is observed. Fully liberated pentlandite grains are common, often with distinctive angular shapes. Fractures are typically present within most grains.

April 28, 2023

7.6   Raman - Mineral analysis

7.6.1   Methodology

For the **Drill Core** sample, the cut surfaces of the supplied core were polished to acquire a smooth flat surface, appropriate for direct **Raman** spectroscopy analysis. The acquisition parameters used varied according to the nature of the minerals under investigation, such that those for opaque minerals were different to those for translucent minerals. For silicates the following parameters were used:

- Laser: 532 nm
- Energy: 25 %
- Acquisition time: 2 sec
- Acquisition accumulation: 3 spectra
- Magnification lenses: 10X

The total acquisition time was 6 sec (2 X 3), where the average spectrum is directly given as final result. These parameters allowed good signal/noise ratio.

For highly light-reflective minerals, such as magnetite or sulphides, a different set of parameters were configured to account for the higher light absorption and minimise noise during acquisition, as follows:

- Laser: 532 nm
- Energy: 10 %
- Acquisition time: 6 sec
- Acquisition accumulation: 3 spectra
- Magnification lenses: 50X

The total acquisition time for this analysis was 18 sec, and magnification was changed to 50X, as this allowed for a better and more detailed spectra acquisition, which was deemed appropriate for acquiring representative spectra.

For the **Run-of-Mine Ore** sample, the same sample preparation was used, by directly polishing a representative piece of crushed ore. Acquisition parameters for the Drill Core were also the same. The **Nickel Concentrate** sample was prepared as a resin-impregnated polished block. Furthermore, a pressed pellet was also made using a binder, and analysed in mapping mode, to acquire and calculate cumulative spectra of the material.

Apart from point analysis, mapping of a c.5 x 4.7 mm area was applied in order to produce mineral/ textural maps as well as to acquire & calculate representative cumulative spectra of the **Drill Core** and **ROM** samples (Energy: 50%, Acquisition Time: 0.25s, Acquisition accumulation: 1 spectra, Magnification lenses: 10X). The **Ni Concentrate** was analysed only by point-based approach due to the nature of the material (no matrix).

It is important to note that Raman mineral identification is based on an RRUF database, which can be used to identify different mineral phases, including those from the same mineral group e.g., amphibole group. Sometimes, however, identification may not be ideal, due to noise in the spectra, or lack of a standard spectrum of the mineral under analysis within the database. For that reason, quality control is required.

April 28, 2023

7.6.2   Results for Drill Core analysis

The Drill Core sample analysed is shown in Figure 12, where it has been placed on a standard thin-section glass slide. Disseminated sulphides are present along with a cross-cutting sulphide-rich veinlet.

Figure 12.
Optical image of the slice of **Drill Core** examined in this Raman test study, showing visible disseminated sulphides within a mafic host rock, cut by a sulphide-bearing veinlet. Mounted onto a glass slide. Length of core shown is approximately 5cm.

Matrix-targeted Test Point Scan

As a first exploratory test, Raman spectra were collected from 50 points, and were designed to cover the main minerals present in the sample. Figure 12 shows the position of those points along with the main 4 phases annotated as follows: amphibole, pyroxene, serpentine and opaque.
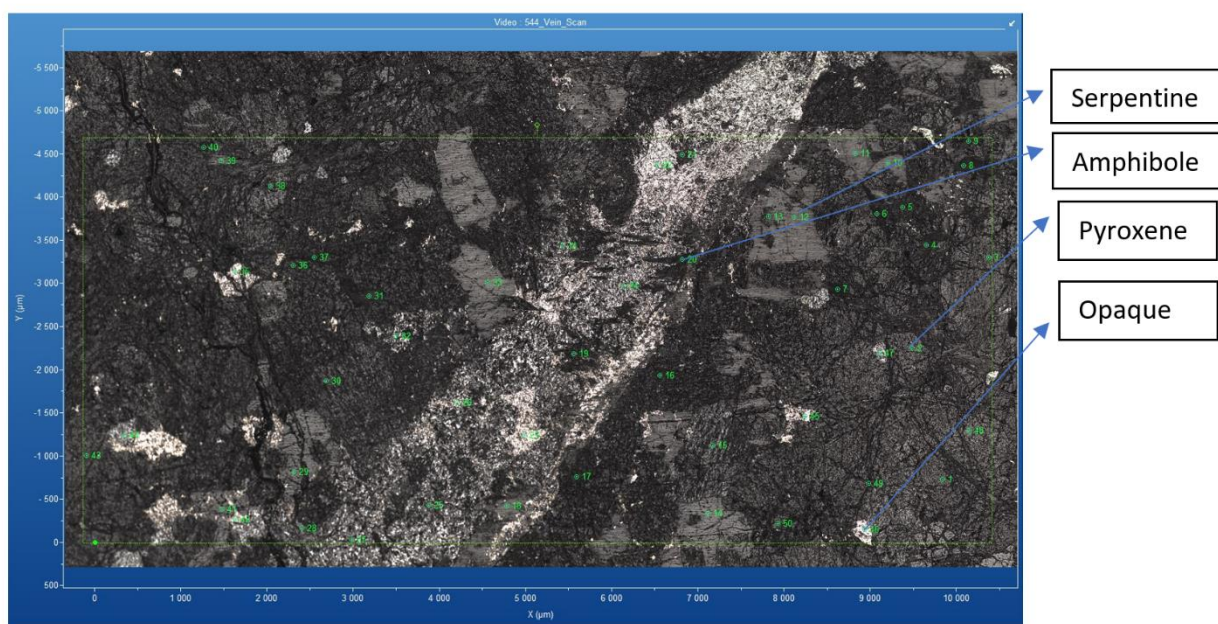
Figure 13.
Drill Core sample imaged at 10x magnification, with Raman point analyses marked as numbers and key mineral phases annotated as Amphibole, Serpentine, Pyroxene and Sulphide (Opaque).

April 28, 2023
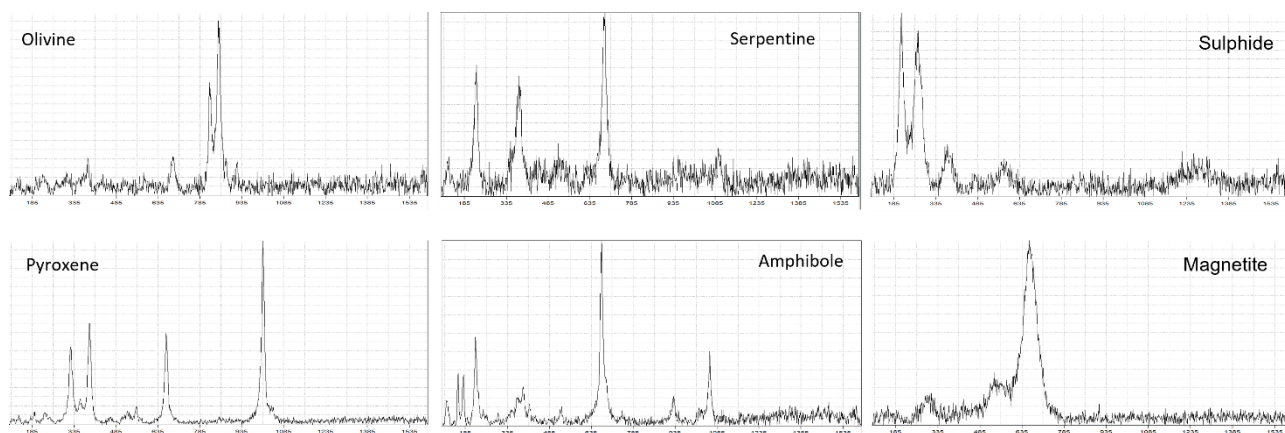
Figure 14.
Example Raman spectra for all the key phases that are present in the **Drill Core** sample illustrating that different minerals have different characteristic Raman spectra.

Vein-targeted Test Point Scan

A similar test analysis was then set-up under a higher magnification setting of 50X, entirely within the vein structure, identifying again the following silicate group minerals: olivine, serpentine and pyroxene. In this case, a better understanding of the textural associations is possible.

Also within the vein are opaque phases and Raman analysis suggests they comprise magnetite and sulphide. The opaque minerals were further investigated outside the veinlet and were also found to be comprising magnetite and sulphide (**Figures 16** & **17**).

Large Area Scan for Cumulative Raman Spectra

A large area was chosen on the **Drill Core** in order to acquire a cumulative Raman spectrum, comprising 200 analysis points, measured over an area of 5 x 10 mm. The results, shown in **Figure 18**, therefore represent an averaged spectral fingerprint of the silicate minerals under examination, where Raman bands can be allocated to the silicate minerals present. Qualitative observation suggests pyroxene dominates the spectrum, followed by amphibole and serpentine.

April 28, 2023
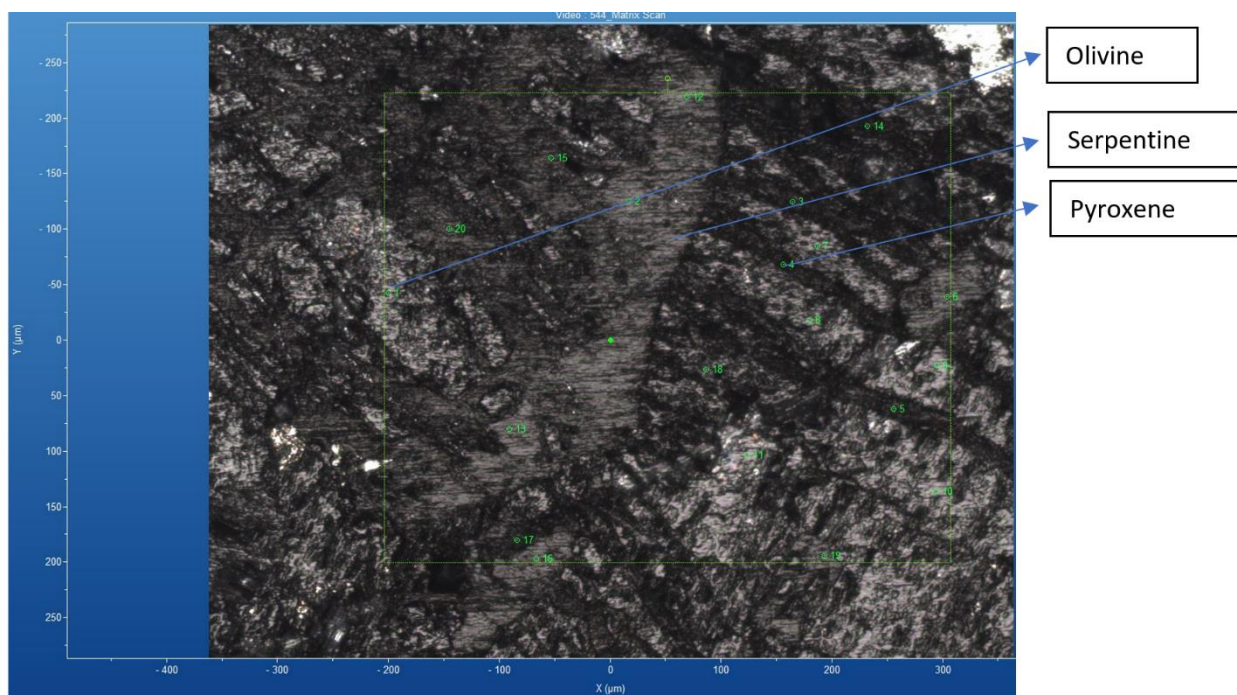
Figure 15.
Raman microscopy image of vein area, at 50X magnification. Numbered points correspond to point analysis, with key mineral phases annotated as Olivine, Serpentine, Pyroxene.
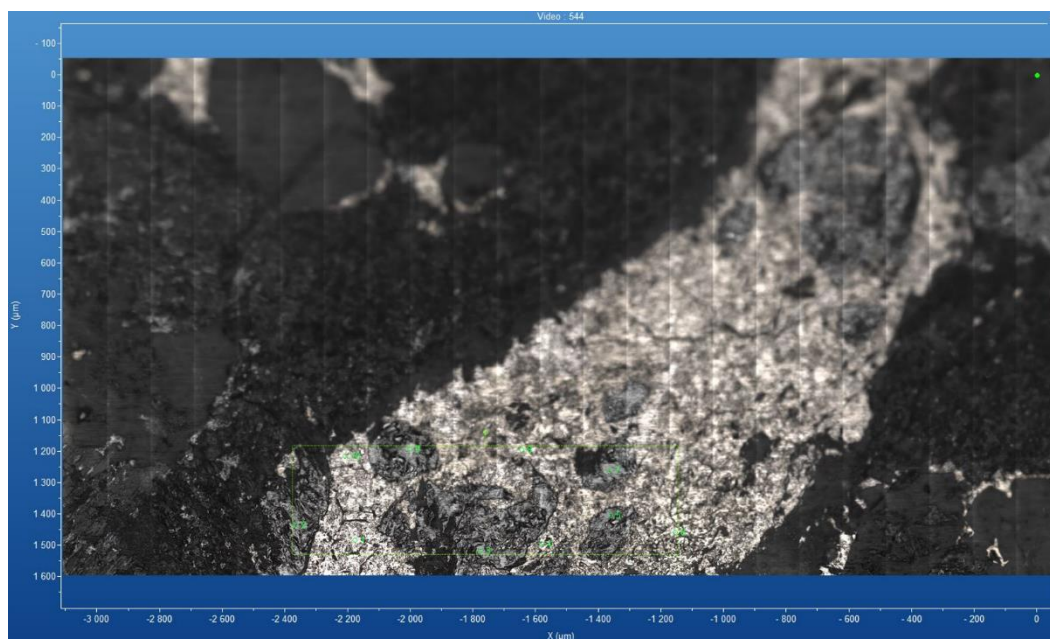
Figure 16.
Raman microscopy image showing detail of the opaque mineral phases within the cross-cutting veinlet.

April 28, 2023
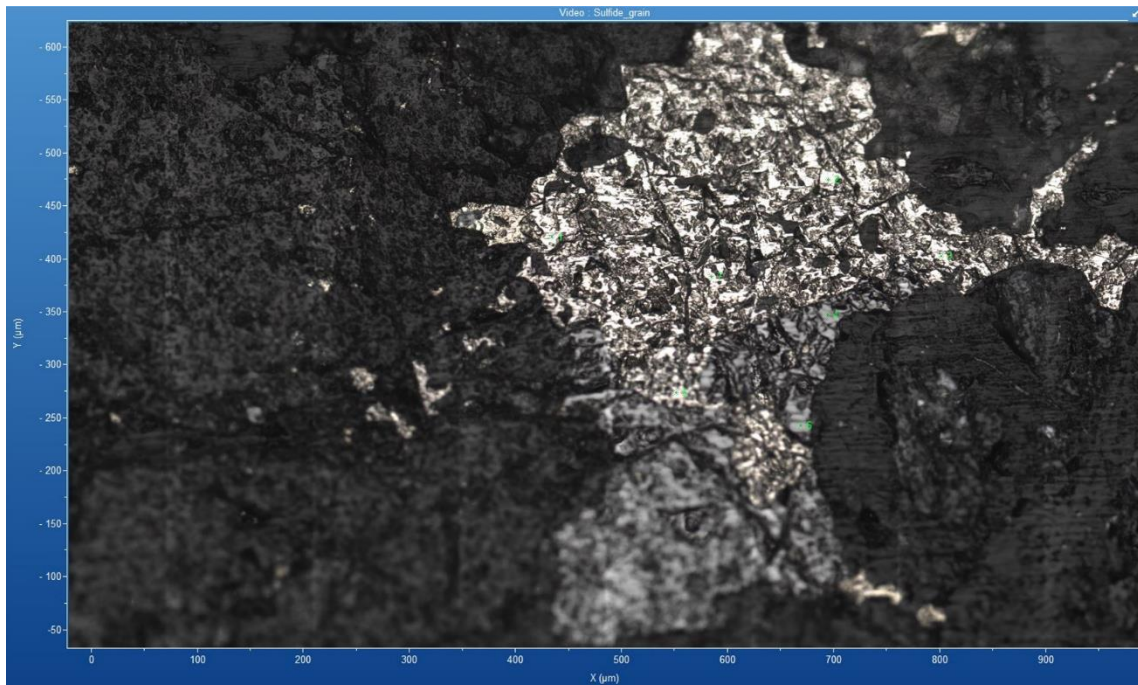
Figure 17.
Raman microscopy image (50X) showing further detail of the opaque mineral phases in the matrix of the sample, and the analysis points selected for investigation.

April 28, 2023
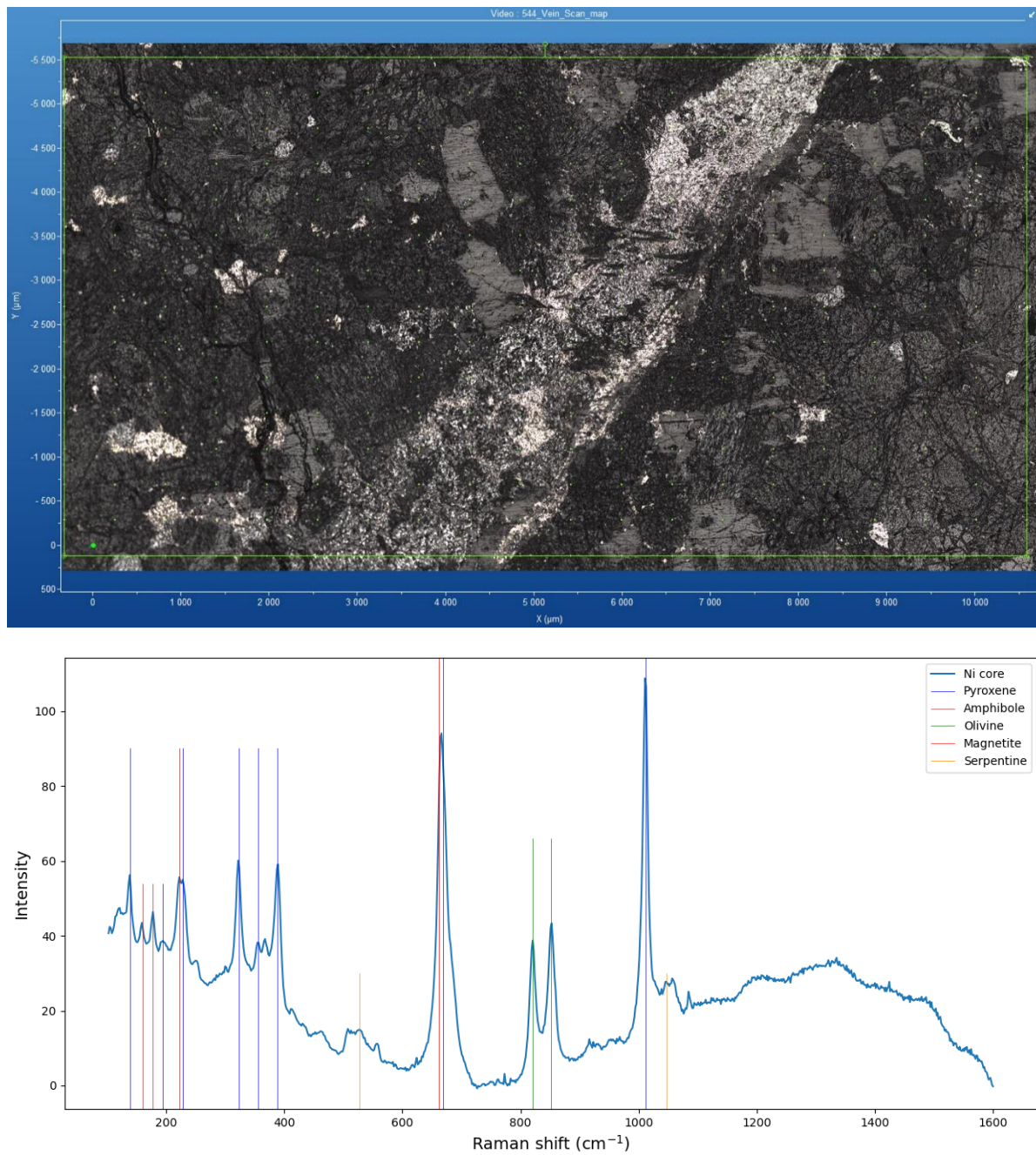
Figure 18.
Cumulative Raman spectrum of an area on the **Drill Core** sample, based on 200 spot analyses (within the area marked on the top optical image), with peaks identified by name and colourized accordingly.

April 28, 2023

7.6.3   Results for ROM analysis
Test areas

A typical **Run-of-Mine Ore** rock chip was chosen for Raman analysis, and then cut and polished (Figure 19). It was noted that this chip had broadly similar textural characteristic to the **Drill Core** examined, including veinlets. A series of point analyses were taken of the surface, and along with pyroxene, amphibole, and serpentine, chlorite was additionally detected. By comparison to the RRUF database, the serpentine was identified as antigorite, the amphibole as actinolite, pyroxene as diopside, and the chlorite as clinochlore.
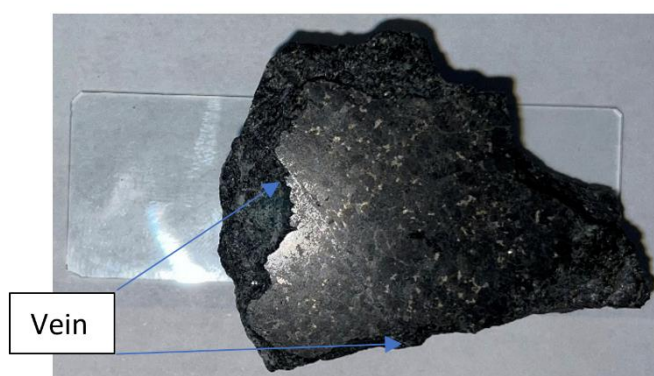
Figure 19.
Run-of-Mine Ore rock chip polished mounted on a standard glass slide for direct Raman analysis.
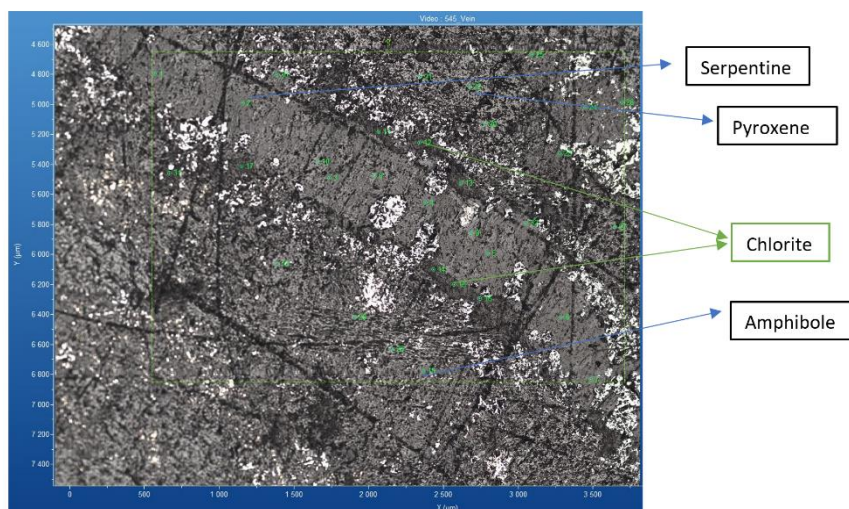
Figure 20.
Point analysis, by Raman, of an area of the polished rock chip sample, with minerals identified.

April 28, 2023

High Resolution Mapping

A high spatial resolution map was then created over an area of 5 x 5mm, consisting of a grid of 9,000 spectral analysis points. The spectral signal of these points was added and averaged to acquire a homogenous spectral fingerprint of the ROM ore sample, as shown in **Figure 21**. It should be noted that the acquisition parameters were most suitable for the silicate minerals rather than the opaque phases.

The interpreted cumulative Raman spectrum shown in **Figure 21**, and by qualitative observation, is noted to be dominated by the presence of pyroxene, followed by serpentine and magnetite. There are bands that could not been attributed to a specific mineral, such as those around 200 cm^{-1}, but most likely these are related to the presence of transitional metals.
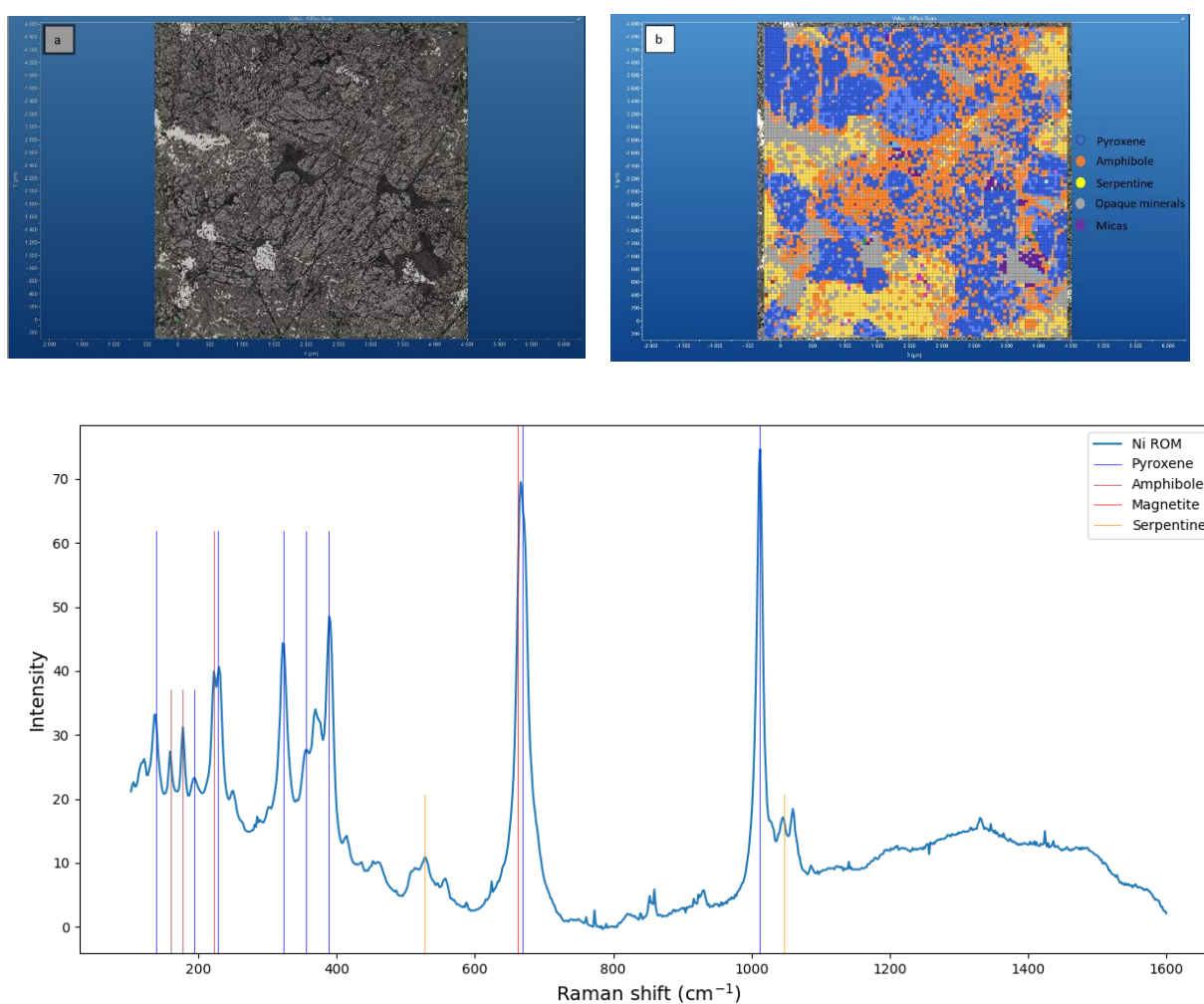
Figure 21.
Cumulative spectra from **Run-of-Mine Ore** sample, created by a grid of 9,000 measurement points, with area of analysis shown in a) above, along with the resulting Raman pixel mineral map in b).

April 28, 2023

7.6.4   Results for Nickel Concentrate analysis

For the **Ni Concentrate** sample, both a pressed pellet and a resin-impregnated block were analysed by Raman. While a pressed pellet can provide a more homogeneous matrix for acquiring and calculating cumulative spectra, a resin block can be utilised for better grain-based analysis on a polished surface, which may prove better for mineral phase characterisation and identification.

Point Scan – resin pack

The **Ni Concentrate** sample is challenging to analyse by Raman because of the fine particle size (typically less than 65μm). Most silicate minerals cannot be fully distinguished from each other, although some spectra from the largest particles suggested they are amphiboles.

On the other hand, sulphidic phases are well distinguished, probably having a variety of composition, encompassing different metals such as Fe, Cu, Ni, Co, interpretation based on the individual Raman spectra analysed. The spectra of those phases, however, are not clear or mono-mineralogical, due to the variable composition within one phase as well as interreference of phases next to the point of analysis.
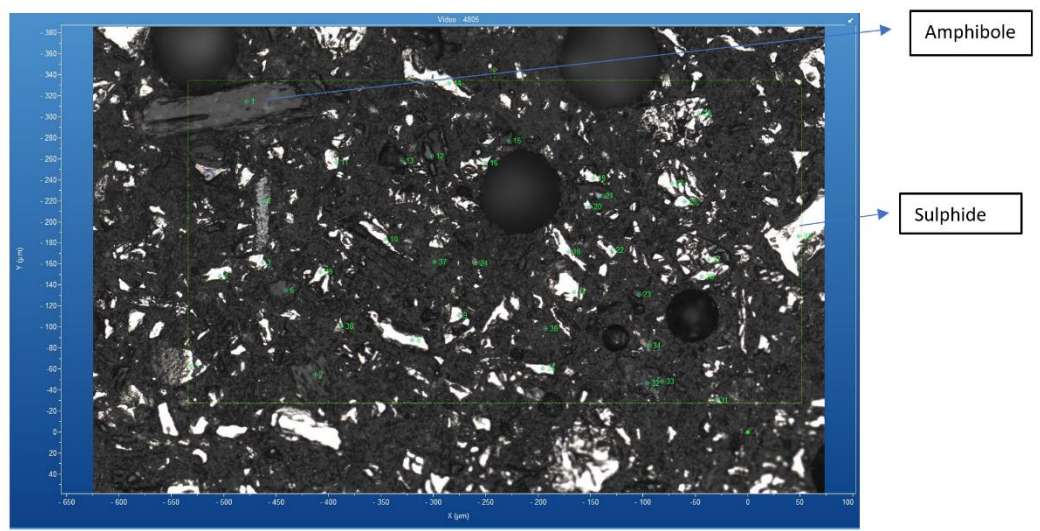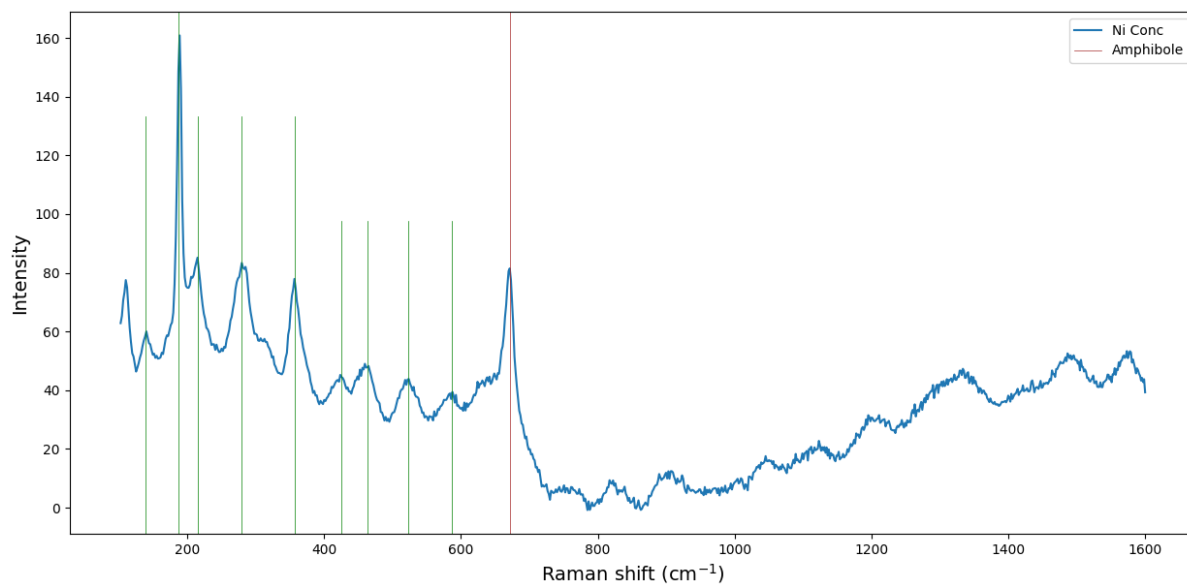

Figure 22.
Raman image of the **Nickel Concentrate** sample which was made into a resin-impregnated block and polished, with points of analysis marked. Magnification x50.

The pressed pellet of the **Nickel Concentrate** sample was used to acquire multiple spectra (208) and construct a spectral fingerprint, as shown in **Figure 23**, where the main peaks are marked, but cannot be fully interpretated because of too many overlapping peaks.

April 28, 2023
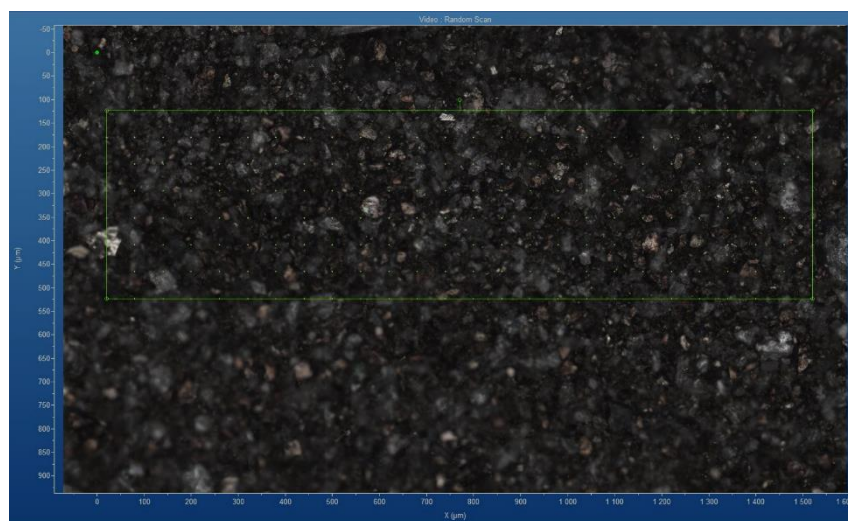
Figure 23.
Cumulative Raman spectra collected from an area of the **Nickel Concentrate** sample (outlined), which was made into a pressed pellet. Magnification x50.

April 28, 2023

7.7 LIBS - Other Mineral Analysis

Laser-Induced Breakdown Spectroscopy (**LIBS**) was selected for this study because of its ability to analyse samples in-situ, and for the ability to take the spectral signature created by the laser and interpret the elemental concentrations, point-by-point. A handheld device was used for this study, and further details are provided in the **Appendix**.

In the case of the **Drill Core** samples, a representative piece was selected, the same piece used for **Raman** analysis, and a polished 2D surface prepared in order to facilitate the spectroscopic analysis. The same was prepared for representative **Run-of-Mine Ore** rock chip samples. In the case of the **Nickel Concentrate**, a pressed powdered pellet with a binder was prepared.

7.7.1 Results for Drill Core analysis

Four phases were investigated by point analysis on phases that could be easily identified by the naked eye, and maps were also created of sulphide-rich areas (**Figure 24**).
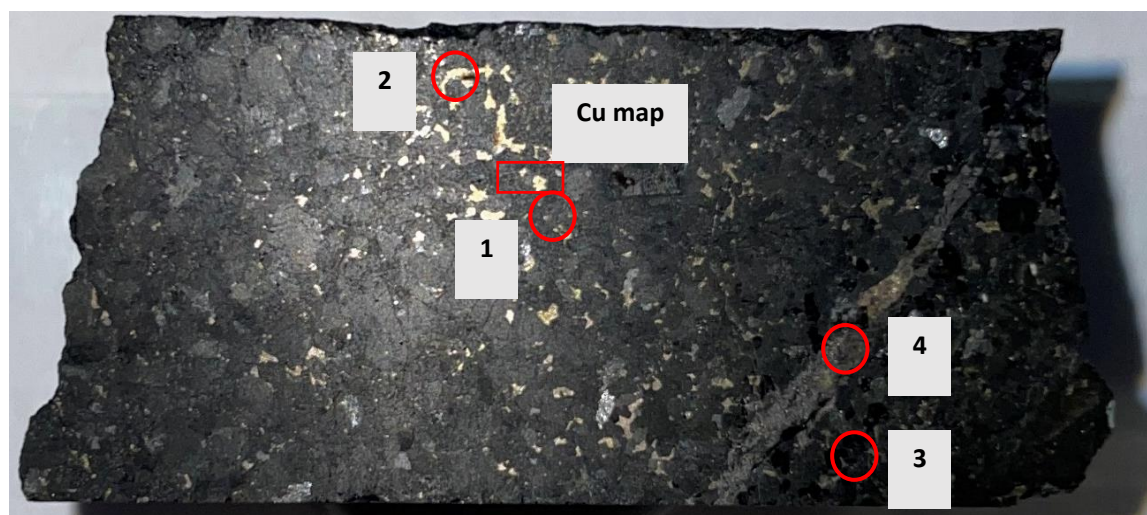
Figure 24.
Optical image of a quarter **Drill Core** sample, as mounted under the LIBS camera. Annotated areas are the spot analyses 1-4 and elemental mapped areas. Length of core is approximately 5cm.

In **Figures 25**-**27**, the **UV-Vis LIBS** and **Vis-IR** spectral range is shown, for the 4 analysed spots on the polished drill core, across the following wavelength ranges: **180-340** nm; **340-600 nm**; and **450-800 nm**.

The **187-600 nm** range is shown in two different graphs, for re-scaling purposes as there is the **340 nm** peak with very high intensity. The peak at **340** nm is thought to be related to phases which contain **Ni** and **Co**, but extra investigation is needed to resolve that combined peak and 'cleaned' from other possible laser oscillation interference.

April 28, 2023

Phase 1 is interpreted to be pyroxene (**Figure 27**), as the spectrum is dominated by the lines of Ca, Mg, Si and Al. **Phase 2** is a sulphide and exhibits the two characteristic peaks of Cu at 324 & 327 nm.

Phase 3 and **Phase 4** are similar with Phase 1 and Phase 2, when compared for the Ca and Mg absorption lines, while for other there is a sequential increasing intensity in specific areas of the spectra. Not all absorption lines are allocated, however, it can be assumed that many of them are secondary lines of primarily Ca and Mg. Further investigation is needed to resolve signal across the observed range of 187-600 nm.

For the Vis-IR spectral range of 450-800 nm as shown in **Figure 27**, more of the major elements are shown, such as Ca, Mg, Na and K. Apart from the annotated lines for each element, the rest is likely related to absorption of different ionization degree of the same elements. **Phase 3** is interpreted to be pyroxene or amphibole, and **Phase 4** may be a mixture (chalcopyrite and silicates).
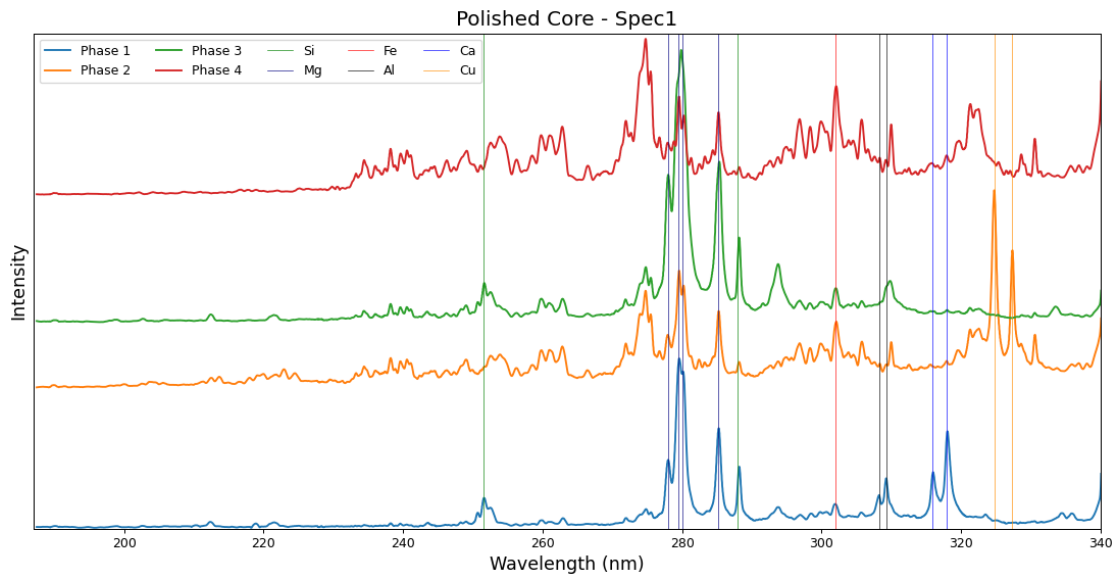
April 28, 2023

Figure 25.
LIBS spectra of the 4 analysed phases in the polished drill core, for the wavelength range of **187-340 nm**.
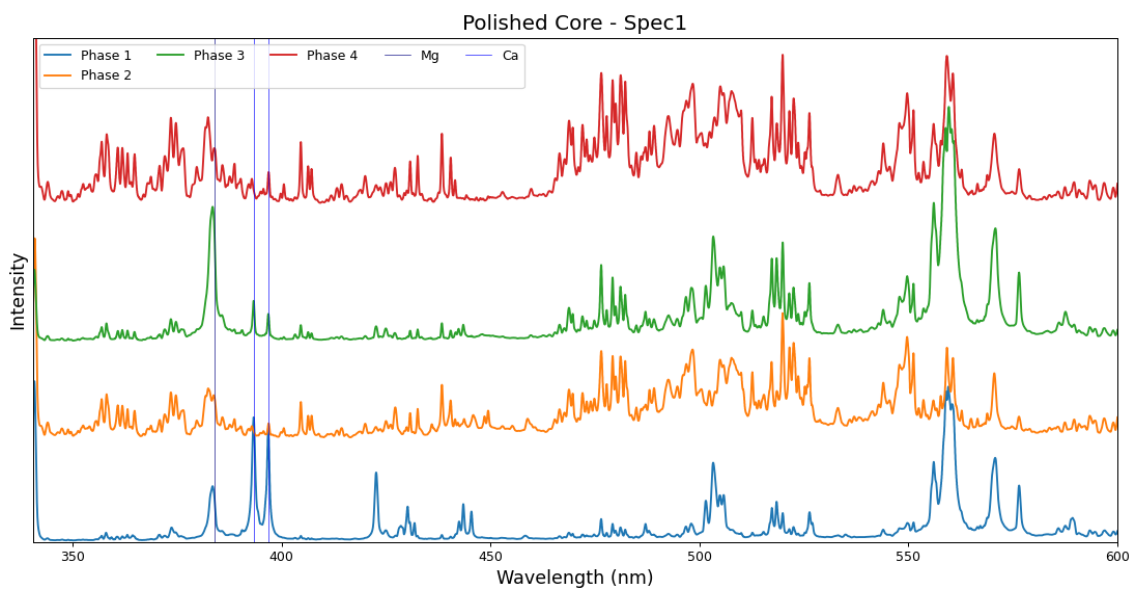

Figure 26.
LIBS spectra of the 4 analysed phases in the polished drill core, for the wavelength range of **340-600 nm**.
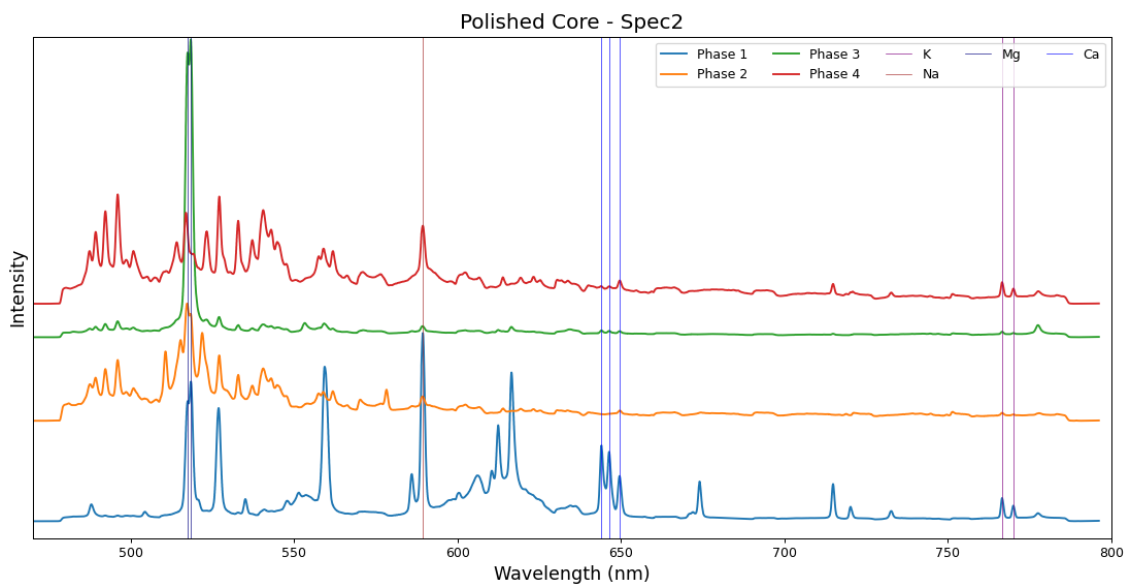
April 28, 2023

Figure 27.
LIBS spectra of the 4 analysed phases in the polished **Drill Core**, for the wavelength range of **450-800 nm**.

A copper map was created across a sulphide grain on a raster basis covering an area of approximately 300 x 300 μm (**Figure 28**). The map is based on the intensity variation of the Cu 327 nm peak across the different mineral phases.

The result suggests that provided any elemental peak is well resolved, and a quantification model exists for the elemental of interest, LIBS can produce qualitative maps of element and metal distribution between phases.
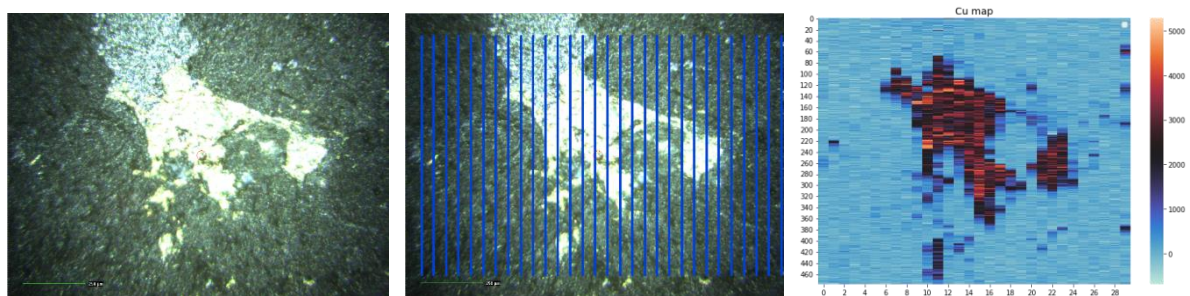

Figure 28.
LIBS copper (Cu) map on a visible copper sulphide grain on the **Drill Core** sample. (a) corresponds to the optical image of the area covered by the map, (b) shows the raster grid placed over the grain, and (c) is the constructed Cu map based on the intensity of the 327 nm peak.

April 28, 2023

7.8　FTIR - Whole-Rock Mineralogical Analysis

The same homogenized powders used for the **QXRD** analysis were further aliquoted and Fourier Transform Infra-Red (**FTIR**) analysis was performed on each of them. This was very much an experimental exercise, such that only qualitative results are possible at this stage, and with the interpretation being guided by the **QXRD** results reported in Section 7.2 above.

The main output from an FTIR analysis is a spectral fingerprint of the sample, and the results for the **Drill Core**, **Run-of-Mine Ore**, and **Nickel Concentrate** are provided in **Figure 29**. The spectra have been processed to take into account the background correction.

The **Nickel Concentrate** sample (green line in **Figure 29**), which is characteristically dark in colour, was found to have a high absorption background above the $1200 cm^{-1}$ wavenumber. This results in an exaggeration of the noise in the spectrum after processing, specifically in the areas of $1500-2000$ cm^{-1}, and >3500 cm^{-1}, but fortunately there appears to be no significant information present in these regions of the spectrum. The **Drill Core** and **Run of Mine Ore** samples (blue and orange line in **Figure 29**, respectively) have lower noise interferences above 1200 cm^{-1} wavenumbers, with significant absorption at 3678 cm^{-1}, likely to be due to the presence of actinolite and or chlorite.
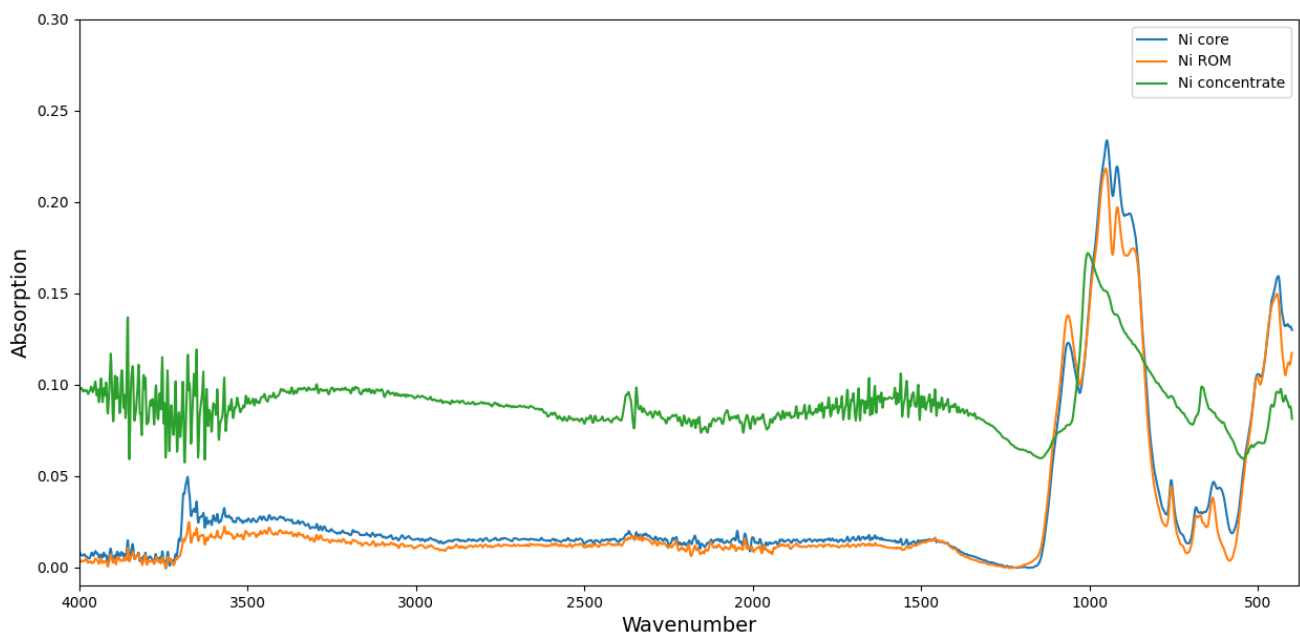

Figure 29.
FTIR spectra for samples of **Drill Core**, **Run of Mine O**re and **Nickel Concentrate**, as acquired within the mid-IR range of 4000-400 wavenumber.

To further investigate the ability of **FTIR** to discriminate minerals present in the samples, a re-scaled (expanded) version of **Figure 29** is shown in **Figure 30**, where an attempt has been made to interpret the information-rich part of the spectra. It appears that pyroxene has the highest influence on the overall FTIR signal, followed by actinolite.

April 28, 2023

Significant overlapping of mineral wavenumbers occurs in the regions of 860-1100 cm^{-1}, as well as <500 cm^{-1}, where Si-O stretching, transformation and bending modes of vibration are known to take place.

In the case of the **Nickel Concentrate** sample, most of the silicate mineral signal is absent, suggesting only minor pyroxene & chlorite, and low talc concentrations occur in the sample. Talc is especially distinctive at the characteristic band of 667 cm^{-1} (grey vertical line in **Figure 30**).

Sulphides such as pentlandite, pyrrhotite and pyrite are usually masked by silicates when present in **FTIR** spectra. However, in the case of the **Nickel Concentrate** sample, which is significantly enriched in sulphides, a distinctive peak can be observed to occur at 1010 cm^{-1} wavenumber. Further calibration is clearly required to positively assign this to the presence of sulphides, and therefore it has not been formally labelled in the figure, but it is encouraging to see such a feature only in this sample which, of the three, is known to contain the most pyrrhotite, pentlandite and pyrite.
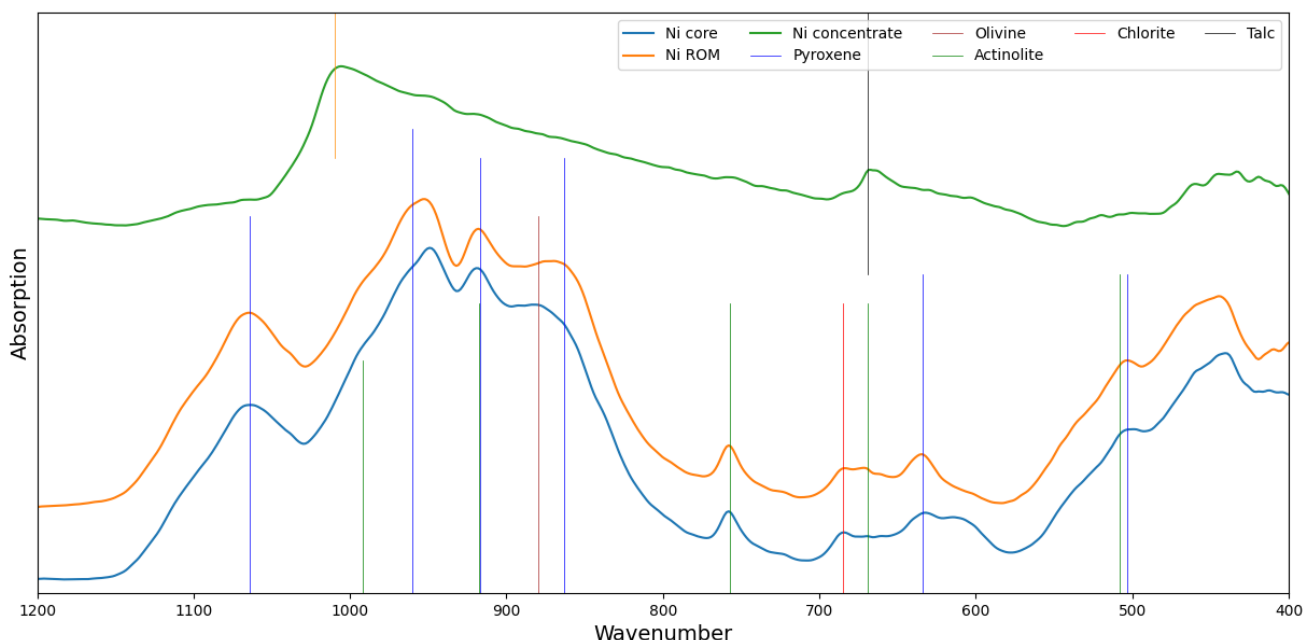

Figure 30.
FTIR spectra for the **Drill Core**, **Run-of-Mine Ore**, and **Nickel Concentrate**, rescaled from **Figure 29**, so as to exaggerate features in the mid-IR range of 1200-400 cm^{-1}. Unique wavenumbers are identified for olivine, pyroxene, chlorite, talc, and actinolite.

8   ACKNOWLEDGEMENTS

April 28, 2023

APPENDIX

A1. QXRD

Whole-Rock fraction XRD method

The samples were first gently disaggregated using a pestle and mortar. After coning and quartering, a 2g split for each sample was micronized in water using a McCrone Micronising Mill to obtain an Quantitative X-Ray Diffraction (QXRD) powder with a mean particle diameter of between 5 - 10 microns. The slurry was dried overnight at 80°C, re-crushed to a fine powder and backpacked into a steel sample holder, producing a randomly orientated sample for presentation to the X-ray beam.

Whole-rock samples were scanned on a PANalytical X'Pert3 diffractometer using a CuKα radiation at 40 kV and 40 mA. The diffractometer is equipped with automatic divergence slits (10 mm irradiated area), sample spinner and PIXcel 1-D detector. Whole-rock samples were scanned from 4.5 to 75° (2θ) at a step size of 0.013 for 4 hours.

The goal of the whole-rock sample preparation is to have a random orientation of the grains, allowing unbiased phase quantification and minimizing the error caused by preferred orientation of certain minerals (e.g. mica flakes, feldspar, amphibole). The study of a randomly oriented powder will give an approximate proportion of clay minerals present in the sample.

Qualitative analysis on whole-rock samples has been carried out using two commercial software packages associated with the ICDD PDF-4 Minerals database: Traces (v.6) by GBC Scientific Equipment and *HighScore Plus* (v.4.9) by PANalytical. For this project QXRD quantitative phase analysis on whole-rock samples has been reported using the Rietveld method with BGMN AutoQuan software.

The Rietveld method is based upon a full-pattern analysis (rather than single peaks) where a computer model allows a theoretical diffractogram to be calculated for any phase mixture. For further detail on the application of the Rietveld method for quantitative mineralogical analysis, see Post and Bish (1989).

Cross validation of XRD analysis with elemental chemistry

A mass balance calculation has been used to validate the mineral quantification given by the Rietveld method. Simplified mineral formulas have been used to calculate the expected bulk chemical composition of the samples from the QXRD mineral quantification and compared with the measured chemical composition from ICP-OES and LECO analyses. The aim of the mass balance calculation is to identify discrepancies between the measured chemical composition of a sample and its mineral content.

The figure below shows the correlation between the chemistry measured by ICP-OES compared to the chemistry calculated by QXRD for the main oxides, using a mass balance approach. For the S content the data obtained by LECO analysis was used instead of the one obtained by ICP-OES because of its higher accuracy.

The match between the actual chemistry and the chemistry calculated by XRD confirms that the quantification of most of the minerals is correct. The good relationship with the calculated Al_2O_3, MgO and SiO_2 confirms the accuracy in the total quantification of quartz, amphibole, serpentine, plagioclase, olivine, pyroxene and talc. The CaO content emphasizes the accuracy of pyroxene, amphibole, and Ca-rich plagioclase quantification.

April 28, 2023

The slight mismatch between the calculated S, from LECO analysis, and the measured one is due to the complexity in the quantification of pyrrhotite by XRD analysis due to the elevated iron content of the samples.

The quantification of **pentlandite** has been verified against the Ni content obtained by ICP-OES. At low concentration there is a good correlation in the quantification of pentlandite between ICP-OES and QXRD while XRD appears to overquantify pentlandite in the concentrate sample. Automated Mineralogy has quantified pentlandite at 22.8% (average of Ni concentrate samples – modal mineralogy mass) and XRD at 22.6% suggesting that the Ni content may be higher than the Ni calibration by ICP-OES.
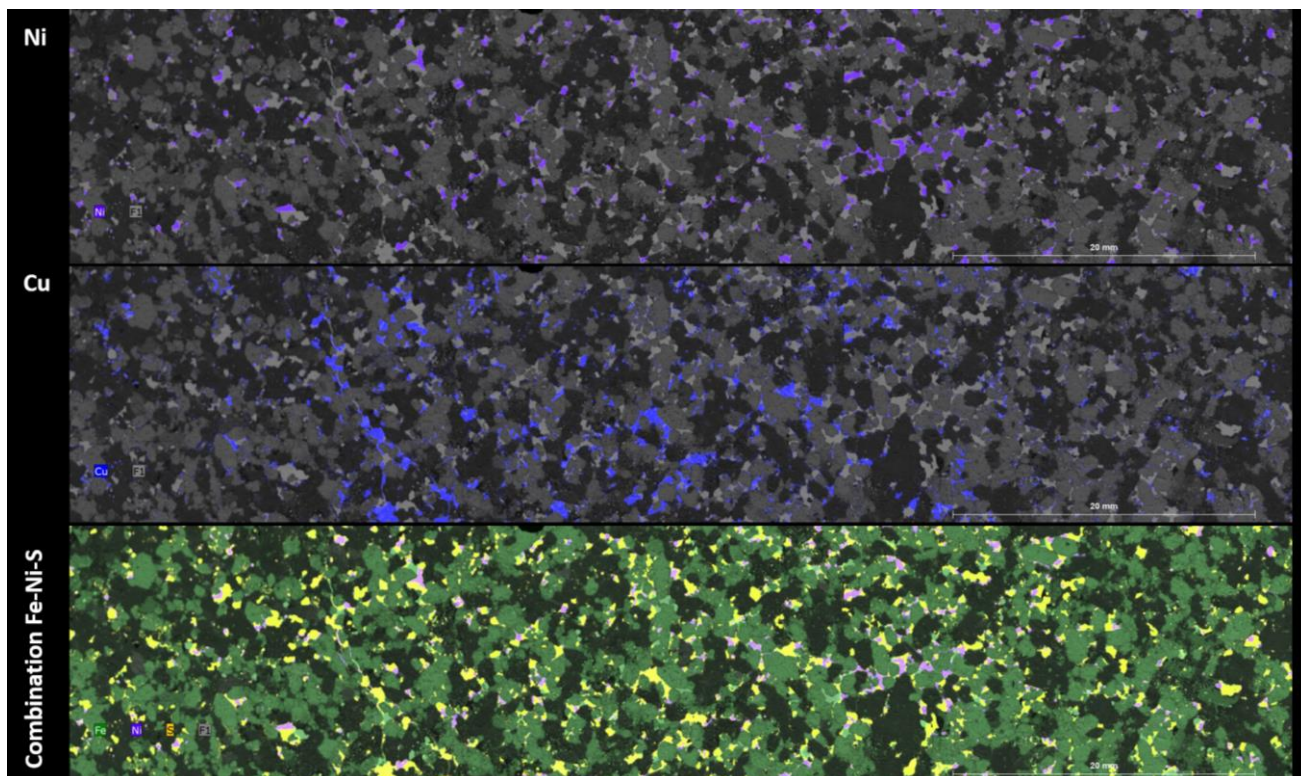
Reference

Post, J.E. and Bish, D.L. (1989). Rietveld Refinement of Crystal Structures Using Powder X-Ray Diffraction Data. *Mineralogical Society of America*, 20, 277–308.

April 28, 2023

A2. Scanning micro-XRF

Drill Core representative of average ore was further investigated by scanning micro-XRF and the resulting elemental maps are provided below for one section of ¼ core.

Extra images of typical **Drill Core** for key elements illustrating pentlandite (Ni map) and chalcopyrite (Cu map) distribution & textures.
F1 refers to the relative intensity of the phases present, based on the average atomic number, and is therefore can be considered a pseudo-BSE value.

April 28, 2023

A3. Automated Mineralogy

The samples were digitally photographed, examined using binocular microscopy and then subsampled. Two approximately 1 g aliquots of the **Nickel Concentrate** sample were dispersed with a filler and then resin impregnated. On curing, the resin blocks were then cross-sectioned and the cross-sectioned surfaces remounted within a resin block, and then polished, so that both areas of the cross section were within the polished face for analysis. This preparation method was used to test for particle segregation within the resin. The surface of the blocks were polished and carbon coated prior to analysis. Two contrasting rock fragments were selected from the **ROM** ore sample. These were embedded in resin and then the surface of the blocks were polished and carbon coated prior to analysis.

The mineral composition and texture of the sample was quantified through automated SEM-EDS analysis (Schultz *et al.*, 2020). Analysis was undertaken using a Hitachi SU3900 scanning electron microscope fitted with a single large area (60 mm²) Bruker SDD energy dispersive spectrometer and running the AMICS automated mineralogy software package. Beam conditions are optimized for analysis and therefore an accelerating voltage of 20kV coupled with a beam current of approximately 15 nA were used. The sample was measured with a segmented field image mode of analysis. This analytical mode subdivides the BSE image into domains (segments) of similar brightness, which represent different particle compositions and then acquires a representative EDS X-ray spectrum from a point within the segment; the phase identified is then assigned to the entire segment. Measurements are optimized to highlight both textural and modal mineralogical information. For the ore concentrate powders an effective image resolution of 1.1 µm is achieved, with 1.6 µm in the ROM ore rock fragments.

April 28, 2023
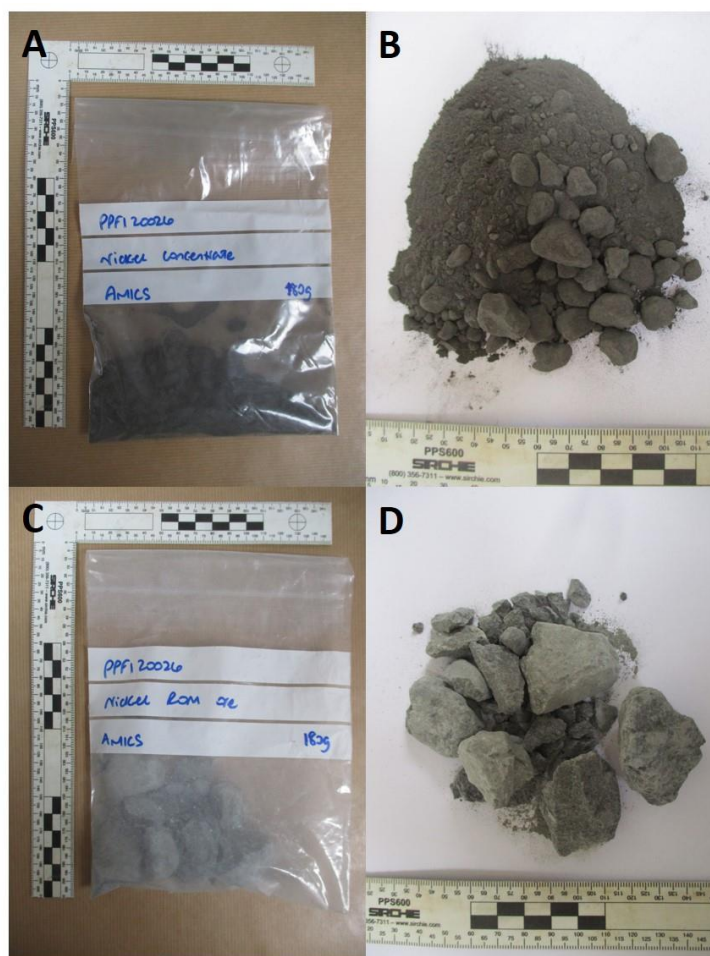
Sample photographs. A, B: Ni Concentrate. C, D: Run-of-Mine ore.

The ED spectra acquired during the measurement are compared with a library of measured and synthetic standards and a phase identification is made on a closest match basis. Phases which are not represented in the standards list at the time of measurement are added either by acquiring reference spectra directly from the sample, or by creating a reference spectrum from the measurement itself. As the standards list can comprise hundreds of reference spectra, the data are grouped into a final, reported compositional list (see table below).

Data outputs include the **AMICS** false colour textural images, along with a full area SEM-BSE montage, which is also captured of the analysed area. Modal abundance data can be expressed as both area % and mass %. Mineral association data for both samples are also provided; these data are based on the measured numbers of transitions between one compositional group and another. Where the association is with "background" it means that the measured phase is adjacent to the mounting medium (resin). Mineral liberation data for the analyses of the Ni concentrate sample are calculated and mineral grain size data (for chalcopyrite, pentlandite and sphalerite) are also calculated.

April 28, 2023

Compositional groupings used to process the data

Mineral	Description
Quartz	Silica group of minerals (e.g. quartz, cristobalite, etc). Includes opal and chert.
K Feldspar	K-rich alkali feldspar including orthoclase, sanidine & microcline.
Plagioclase	Na-rich plagioclase such as albite and oligoclase.
Calcic Plagioclase	Ca-rich plagioclase such as labradorite and bytownite.
Muscovite	Muscovite and Al-rich white mica such as sericite.
Biotite & Phlogopite	Biotite. May include Ti-bearing mica varieties. Also includes Mg-rich micas such as phlogopite.
Kaolinite	Kaolinite and dickite.
Chlorite & Vermiculite	Mostly vermiculite but may include Mg-rich chlorite compositions of chlorite and Al-rich orthorhombic amphiboles.
Olivine	Olivine. May be zoned with Mg-rich / Fe-poor cores and Fe-bearing rims.
Orthopyroxene	Mg-rich orthopyroxene compositions such as enstatite and bronzite. May also include Mg-rich orthoamphiboles such as anthophyllite as well as talc.
Serpentine	Mg-rich silicates such as serpentinite.
Clinopyroxene	Mg-rich clinopyroxene compositions such as diopside. Contains little or no Al.
Clinopyroxene (Mid Al)	Al-bearing Mg-rich clinopyroxene and clinoamphibole.
Clinopyroxene (High Al)	Al-rich clinopyroxene and clinoamphibole.
Zoisite	Ca Al silicates such as zoisite, epidote and prehnite. May also include trace amounts of anorthite.
Calcite	Calcite and ferroan calcite.
Dolomite	Dolomite and ferroan dolomite. Also includes magnesite and / or brucite.
Fe Oxides	Fe oxides such as magnetite (often Ti-bearing) and hematite.
Ti Oxides	Ti oxides such as ilmenite, rutile and anatase. Also includes titanite and perovskite.
Cr Spinel	Chromite and chrome spinel.
Pyrite	Pyrite and marcasite.
Pyrrhotite	Pyrrhotite and troilite.
Chalcopyrite	Chalcopyrite. May also include other Cu sulphides such as bornite and chalcocite.
Pentlandite	Ni sulphides. Mainly pentlandite but may include small amounts of makinawite, violarite etc.
Sphalerite	Sphalerite and other Zn sulphides.
Sulphates & Phosphates	Sulphates such as gypsum and phosphates such as apatite.
Zircon	Zircon, monazite and other HFSE or REE-bearing minerals.
Undifferentiated	Phases not included in the above categories.

Reference

SCHULTZ, B., SANDMANN, D. & GILBRICHT, S. 2020. SEM-based automated mineralogy and its application in geo- and material sciences. *Minerals*, **10**, 1004; doi:10.3390/min10111004.

April 28, 2023

A.4 LIBS

LIBS analysis parameters for the 3 different samples, either presented as a 2D polished rock surface or pressed pellet were:

- Spectral resolution (Grating): 1200
- Gate Delay and gate width: 0.11 & 3 µsec
- Energy at 70%
- Number of shots: 200 @ 40Hz repetition rate
- Spot size 30um

The LIBS instrument used in this study has two detectors for UV-Vis (Spec 1: 187-600 nm) and Vis-IR (Spec 2: 450 – 800 nm), and therefore a 10-spot analysis protocol was devised for acquiring a full spectrum analysis for the samples.

Analysis conducted on the polished core and ROM was focused on pointing and shooting at different phases that were observed and identified by eye, whereas for the pellet analysis, full spectra were acquired from representative areas of the pellet's surface.

April 28, 2023

End of Report